

Project: A healthy society - towards the optimal management of wind turbine noise



D3.1 Complete review of the existing methods and models of infrasounds' measurement and impact on human health (M6)



Projekt: Healthy society - towards optimal management of wind turbines' noise



Państwowy
Instytut
Badawczy



INSTYTUT MEDYCYNY PRACY IM. PROF. J. NOFERA



D3.1 Complete review of the existing methods and models of infrasounds' measurement and impact on human health (M6)

Executive summary

Wind turbines generate aerodynamic noise, one of whose components is low frequency noise. In order to accurately characterize the noise measured in the vicinity of wind farms, it is necessary to ensure that outdoor microphones are adequately protected from the wind. The measurement of infrasound at low levels requires a specific methodology too, as it is readily affected by the wind on the microphone in low frequencies. Such a methodology has been tested in a few countries such as Japan, Australia, Belgium, USA and Denmark.

A comprehensive review of the literature was also carried out on the impact of low frequencies, particularly infrasound, on mental health, brain morphology and other aspects of human well-being. Despite strong indications regarding the effects of infrasound on mental health and cognitive functions in humans, there are virtually no studies that directly investigate infrasound effects on human health in a randomized and controlled manner.

After conducting a literature review about infrasounds models, it can be stated that the most frequently used methods for predicting infra and low frequency noise (LFN) generated by wind turbines are the methods generally used for predicting environmental noise, i.e. the method described in ISO 9613-2, the CNOSSOS method and the NORD2000 method despite the fact that more sophisticated techniques for LFN prediction can be found in the literature.

Authors	Date of submission	Confidentiality level
Tadeusz Wszolek Maciej Kłaczyński Paweł Małecki Dominik Mleczko Paweł Pawlik Bartłomiej Stępień	30.IX.2021	It can be made available on the project website: https://hetman-wind.ios.edu.pl

1. Noise sources in wind turbines

Wind turbines generate two types of noise, mechanical noise and aerodynamic noise.

The sources of mechanical noise are: electric motor, gearbox, yaw motor (Figure 1). The mechanical noise produced by shafts and gears can be propagated to the environment through the elements of the turbine structure such as: the nacelle, hub, rotor, and tower (Figure 1).

Examples of sound power values for individual turbine components are presented in (Pinder, 1992; Wagn, BareiB and Guidati, 1996; Pantazopoulou, 2009).

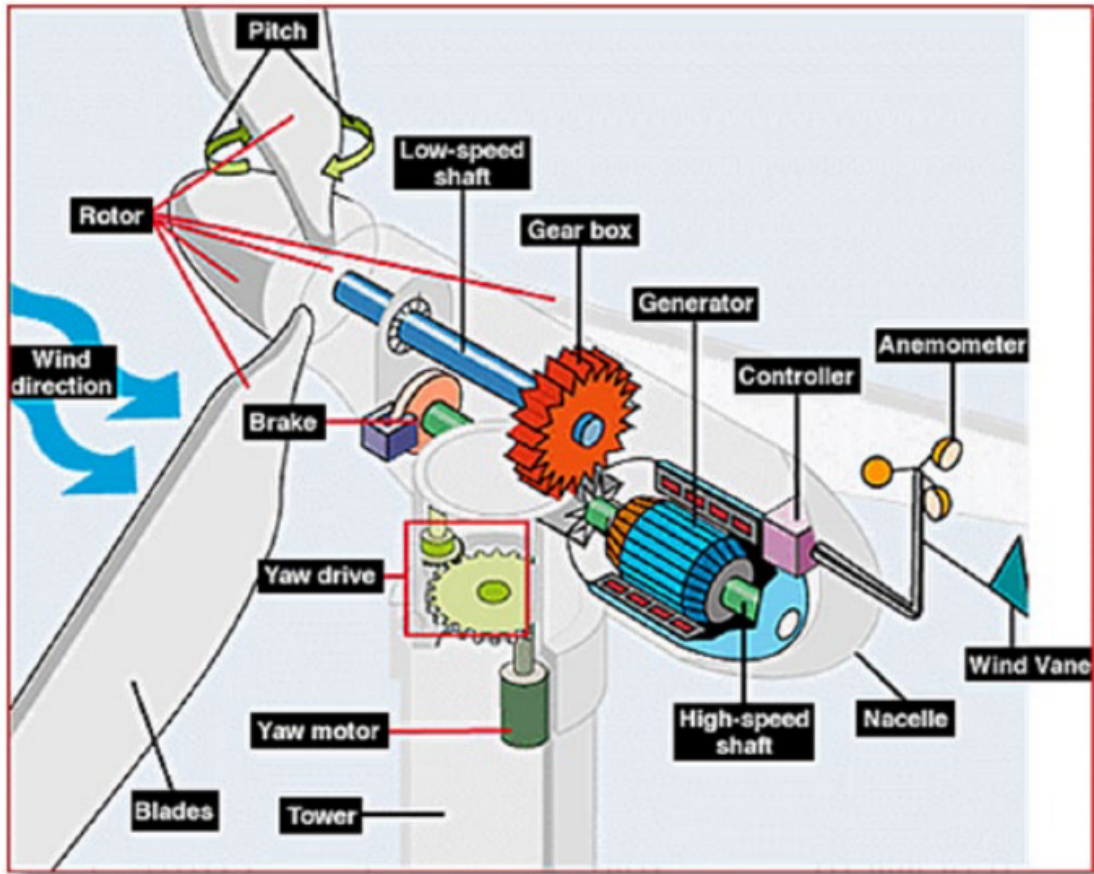


Figure 1. Components of a wind turbine. Source: US Department of Energy (Raman, Ramachandran and Aldeman, 2016)

For large wind turbines in the 1-6MW range, the rotor with blades rotates at 10-22 RPM (Raman, Ramachandran and Aldeman, 2016), this corresponds to frequency values of 0.16-0.36Hz. Multiplying this value by the number of blades (3) gives a blade frequency in the range from 0.48-1.08Hz. The blade frequencies and their harmonics can be observed in the acoustic signal. An example of the sound pressure level spectrum is presented recorded at a distance of 622 meters from the turbine is shown in Figure 2.

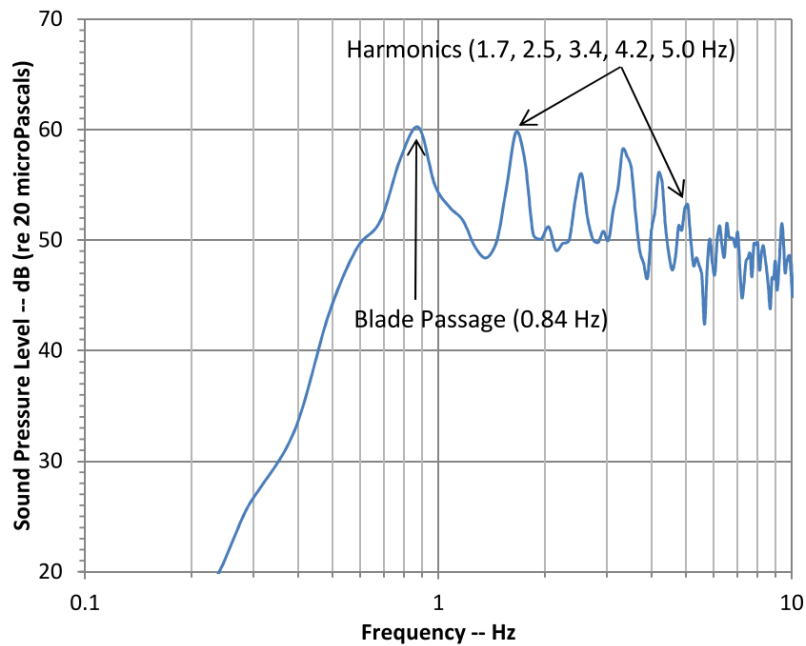


Figure 2. Spectrum of wind turbine infrasound at a distance of 622 meters (Carman, 2015)

For geared turbines, 90:1 gear ratios are typically used (Zipp, 2012)(Hu, 2018), which increase the rotational speed to a range of 900-1980 RMP, this corresponds to frequencies in the range of 15-33Hz. There are also turbines with 30:1 gear ratios, where the last gear ratio step is abandoned. For large multimegawatt wind turbines, the gearbox is abandoned and the generator rotor rotates at the same speed as the turbine rotor.

The generator shaft frequency can be observed in the acoustic signal spectrum for Upwind Rotor turbines (Figure 3)(Hubbard and Shepherd, 2009).

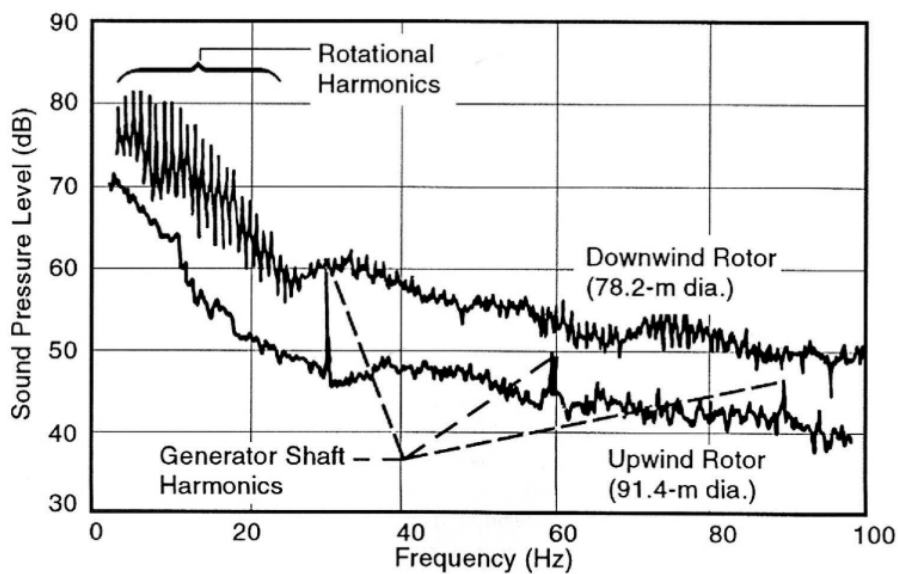


Figure 3. Low-frequency, narrow-band noise spectra from large-scale HAWTs with upwind and downwind rotors. (bandwidth = 0.25 Hz, distance = 150 m) (Hubbard and Shepherd, 2009)

Aerodynamic sound generally increases with rotor speed, and the noise-producing mechanisms can be divided into three groups (Kłaczyński and Wszolek, 2014):

- Low frequency noise, related to the low (below 200 Hz) frequency of spectrum. It occurs mainly when the rotating rotor blades encounter local air gaps associated with the flow around the tower or change of wind speed;
- Inflow turbulence noise, which appears as a result of turbulence or local pressure fluctuations around the rotor blades;
- Airfoil self noise, an aerodynamic phenomenon that occurs along the blades. This noise is wideband but it also occurs in the form of tone, mainly due to the blunt end of the wing and the air-flow through exist slits and holes. With a favourable wind, the rotor blade's tip can move at a speed of 250 km/h (about 70 m/s), resulting in the emission of sound with distinct tonal components in the frequency range of 700–800 Hz (Kłaczyński and Wszolek, 2014).

2. Measurement and assessments of infrasound and low frequency

Infrasound is generated also by a range of natural sources, including waves on the coastline, waterfalls and wind. It is as well generated by a wide range of man-made sources such as industrial processes, vehicles, air conditioning and the wind turbines discussed above. The measurement of infrasound at low levels requires a specific methodology, as it is readily affected by wind on the microphone. Such a methodology has been tested (developed) in few countries.

Hideki TACHIBANA, Japan

In the Wind Turbine Noise (WTN) problem, the effect of low frequency components including infrasound is an important matter of controversy, and therefore prototype wide-frequency-range sound level meters with a measurement frequency range from 1 Hz to 20 kHz and a function for recording the sound pressure signal were used. To prevent wind-induced noise at a microphone particularly at low frequencies, a prototype wind-screen set shown in Figure 4 was devised. This set is of a double-skin type consisting of a globular wind-screen of 20 cm diameter made of urethane foam and a newly designed dodecahedral second screen covered with a thin cloth (nylon 90% and polyurethane 10%; opening ratio: 60%) with high elasticity. The insertion loss of this wind-screen set is below 1 dB up to 4 kHz as a result of measurement in anechoic room. Its wind-shielding effect was checked by a field measurement in a very quiet plain

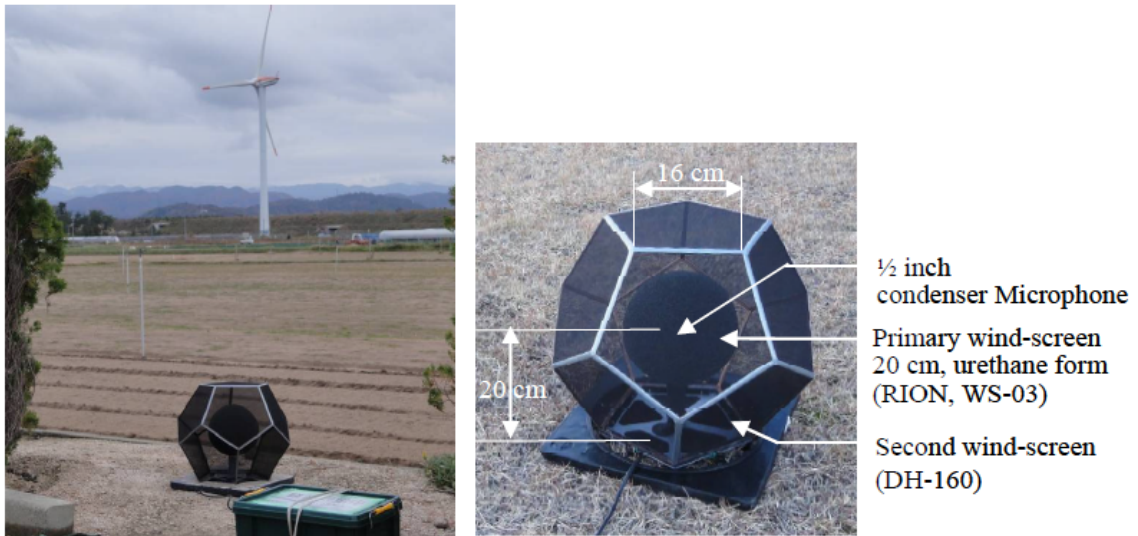


Figure 4. An example of field measurement using the double-skin type wind-screen (Tachibana, 2014)

Acoustical characteristics of WTN: From the measurement results obtained at 164 points in the residential areas around 29 wind farms, it was found that WTN generally has a spectrum characteristic of about - 4 dB/octave in band spectrum and the components in the infrasound frequency region were much below the hearing thresholds. This fact was examined through a laboratory experiment conducted as part of this research project (Yokoyama, Sakamoto and Tachibana, 2013). These indicate that WTN is not a problem in the infrasound frequency region. However, most of the frequency components in audible frequency range are above the hearing thresholds. This means that WTN should be discussed as an “audible” environmental noise.

Turnbull CP, Turner JP, Australia

A microphone mounting method is provided in IEC 61400-11. The method was developed to minimise the influence of wind on the microphone for the measurement of noise in frequencies higher than those associated with infrasound. This is achieved by mounting the microphone at ground level on a reflecting surface and by protecting the microphone with two windshields constructed from open cell foam. The method was not developed specifically for the measurement of infrasound, and wind gusts can be clearly detected when measuring in the infrasound frequency range using the above method. Therefore, this study has developed an alternative method to reduce the influence of wind on the microphone that would otherwise mask the infrasound from the turbine. A below ground surface method was developed based on a similar methodology (Betke K, Schults von Glahn M and Goos O, 1996). This method has been adapted for this study, and includes a dual windshield arrangement, with an open cell foam layer mounted over a test chamber and a 90mm diameter primary windshield used around the microphone. Methodology is based on measurements being conducted below the ground surface in a test chamber that is approximately 500mm square and 500mm deep to reduce the influence that even light surface breezes can have on the infrasound results. The below ground methodology has been tested and it has been confirmed that levels of infrasound above the ground and within the chamber are the same in the absence of surface winds when measuring a known and constant source of infrasound.

The microphone mounting arrangement is depicted in Figure 5.

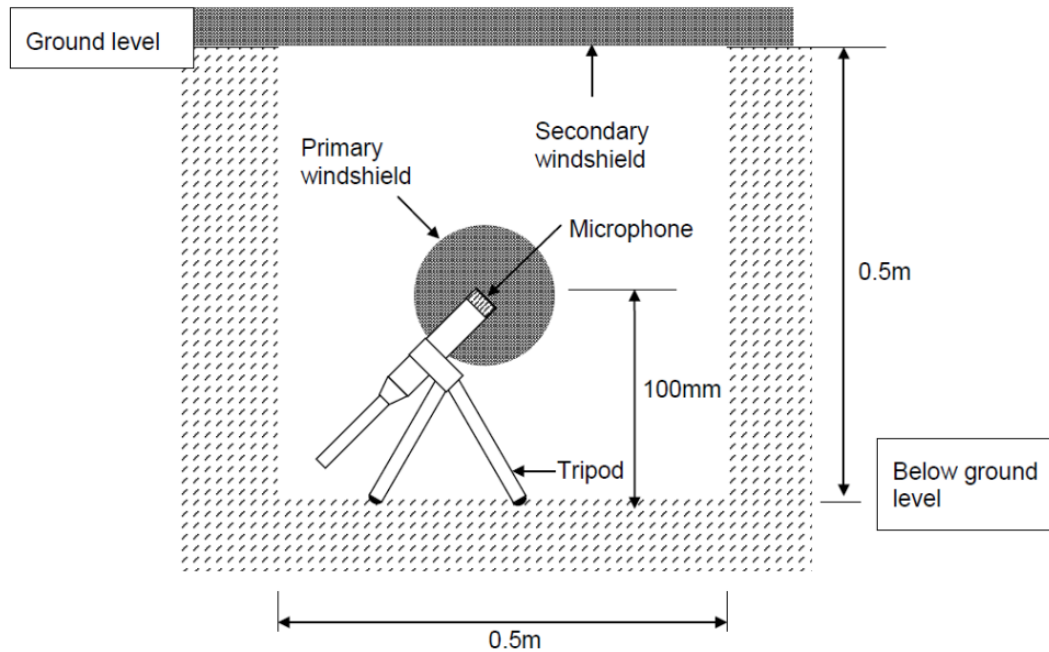


Figure 5. Schematic of Microphone Position (not to scale) (Turnbull CP, 2011)

Infrasound was measured using the below ground methodology at two Australian wind farms, Clements Gap in the mid-north of South Australia and Cape Bridgewater in the coastal region of south-western Victoria. Infrasound was also measured in the vicinity of a beach, a coastal cliff, the city of Adelaide and a power station using the below ground methodology. The measured levels of infrasound from the wind farms have been compared with the other natural and man-made noise sources and all measurements have been compared with recognised audibility thresholds. Infrasound is generally considered to be sound at frequencies less than 20 Hz and is often described as inaudible, However, sound below 20 Hz remains audible provided that the sound level is sufficiently high (O’Neal, Hellweg and Lampeter, 2009). The thresholds of audibility for infrasound have been determined in a range of studies (Leventhall, Pelmeare and Benton, 2003). The G-weighting has been standardised to determine the human perception and annoyance due to noise that lies within the infrasound frequency range (ISO 7196:1995, no date). A common audibility threshold from the range of studies is an infrasound level of 85 dB(G) or greater. The audibility threshold limit of 85 dB(G) is consistent with other European standards and studies, including the UK Department for Environment, Food and Rural Affairs threshold developed in 2003 (Leventhall, Pelmeare and Benton, 2003), the UK Department of Trade and Industry study (Hayes McKenzie Partnership, 2006), the German Standard DIN 45680 (DIN 45680, 1997) and independent research conducted by Watanabe and Moeller (Watanabe and Møller, 1990). The generation of infrasound was detected on early turbine designs, which incorporated the blades ‘downwind’ of the tower structure (Hubbard and Shepherd, 1990). The mechanism for the generation was the blade passing through the wake caused by the presence of the tower.

Kristy Hansen, Branko Zajamšek, Colin Hansen, Australia

In order to accurately characterise the noise measured in the vicinity of wind farms, it is necessary to ensure that outdoor microphones are adequately protected from the wind. A standard 90mm windshield is appropriate for measurements in light winds; however, as the wind speed increases, wind-induced pressure fluctuations erroneously contribute to the measured sound pressure level. Three alternative secondary windshields have been developed and tested in an outdoor environment and evaluated for their ability to allow low frequency noise and infrasound measurements to be obtained in the presence of wind. In addition, the effect of the microphone location with respect to the ground surface has been investigated for frequencies up to 1000 Hz. The measured sound pressure levels have been compared through analysis of high resolution frequency spectra and coherence for various wind conditions. Results show the presence of the wind turbine blade-pass frequency and its harmonics in the infrasonic range. In the low-frequency range, broadband peaks with superimposed secondary peaks spaced at the blade-pass frequency are evident. These spectral characteristics are further accentuated by stable atmospheric conditions. Results at low wind speed are also analysed to investigate the pressure doubling effect, in the context of low frequency noise, for all microphone mounting configurations. Comparison between the results using microphones with different secondary windshields mounted at ground level, at 1.5m and sub-surface in a box shows that there is no consistent difference between measurements below 100Hz. This indicates that the 6dB correction may be relevant for any microphone location within a quarter of a wavelength from the ground.

All three outdoor microphones were equipped with 90mm-diameter windshields as well as secondary windshields of various configurations. One microphone was positioned at ground level, another was mounted at a height of 1.5m, and the third was located underground inside a small plywood box. The microphone at ground level pictured in Figure 6b was taped horizontally at the centre of a 1m diameter aluminium plate of 3mm thickness and covered by both a primary and secondary windshield as specified in the IEC 61400-11 standard. The secondary windshield consisted of a 16mm layer of acoustic foam, covered by a layer of SoundMaster acoustic fur. The windshield was riveted to the aluminium plate and secured with a pin. The microphone pictured in Figure 6d was mounted at a height of 1.5m using a stardropper to minimise wind noise interference associated with the more conventional method of tripod mounting. This microphone was fitted with a secondary spherical windshield which was attached to a steel frame of diameter 450mm as shown in Figure 6d. The windshield materials were identical to those used for the hemispherical secondary windshield described above.

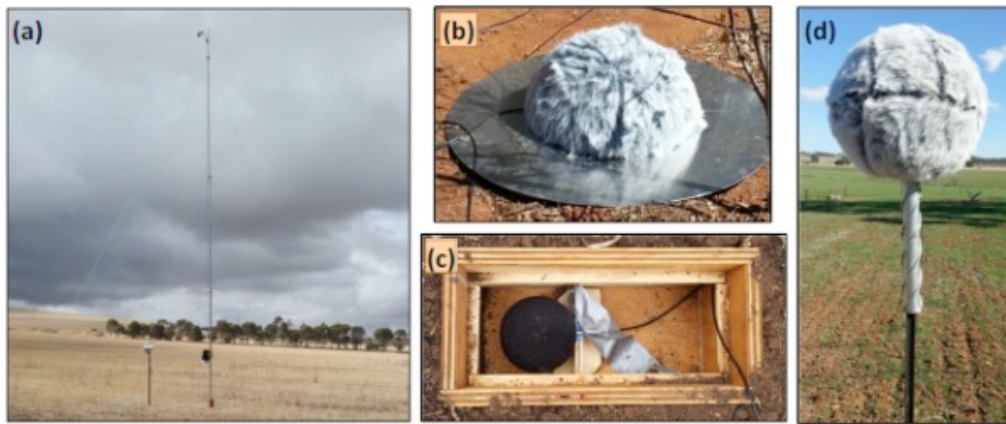


Figure 6. (a) Davis weather stations at 1.5m and 10m, (b) Hemispherical windshield, (c) box windshield and (d) spherical windshield (Hansen, 2013)

Sarah D'Amico, Timothy Van Renterghem, Dick Botteldooren, Belgium

Wind-induced microphone noise complicates infrasound measurements considerably. A wind-shielding dome for signal-to-noise ratio improvement of acoustic pressure infrasound frequencies was designed and tested. The semi-spherical shape aimed at maximizing the pressure averaging of large atmospheric turbulent eddies while keeping the structure reasonably compact. The insertion loss of the dome was measured in a semi-anechoic chamber (in absence of flow) and showed nearly full transparency in the low frequency range. In an outdoor test, wind turbine infrasound was simultaneously measured with an uncovered and a dome-covered low-frequency microphone under different wind speeds and turbulence intensities. Largest improvements of the signal-to-noise ratio were measured at high mean wind speeds for frequencies down to 0.5 Hz. The dome allowed to clearly identify the infrasonic tonal components of wind turbines that were otherwise completely covered by the wind-induced microphone noise even at low mean wind speeds. The use of the dome thus opens possibilities for more accurately measuring infrasonic immissions from e.g. wind turbines.

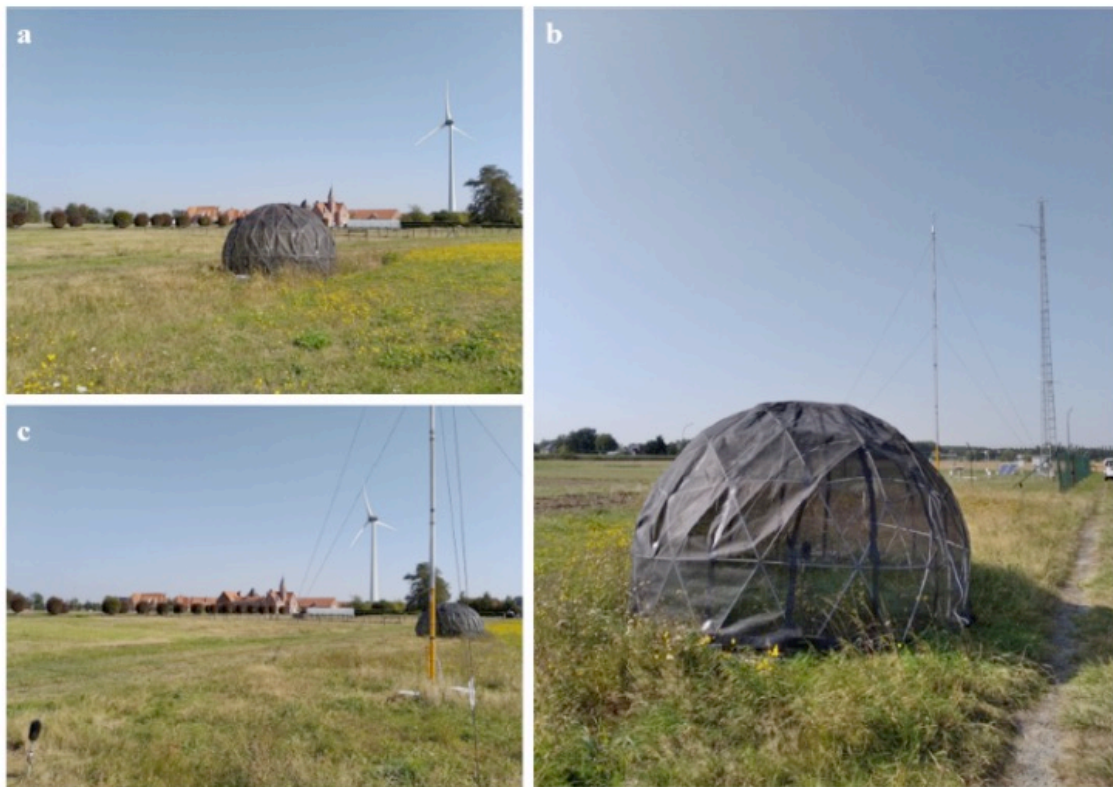


Figure 7. Wind domes (D'Amico, Van Renterghem and Botteldooren, 2021)

A wind-shielding hemi-spherical dome for improving SNR for outdoor measurements of infrasound was designed and tested in detail. The shape of the structure and the porosity of the wind breaking textile were based on findings reported in literature and theoretical considerations regarding wind fence enclosures. The dome was shown to be nearly acoustically transparent in the low frequency range tested and within the limits of the experimental setup indoors. In an extensive outdoor test, the dome showed to reduce wind-induced microphone noise in the infrasonic spectral range down to a characteristic-length ratio of 0.2 or 0.5 Hz. The wind-shielding dome allowed to clearly identify the tonal components in the infrasonic frequency range from wind turbines at close distance. At the non-dome covered microphone, these tones are mostly submersed in wind-induced microphone noise. Even at low mean wind speeds, the infrasonic wind-induced microphone noise at the non-dome covered microphone (but still with a standard 10-cm diameter spherical foam windscreen) shows to be strongly influenced by the turbulence intensity in the wind flow. The SNR is thus significantly improved by the dome, allowing to reveal the BPF and its harmonics, also at high TIs. Maximum improvement of the SNR was seen for the case of 6 m/s mean wind speed at different TIs, occurring at approximately 1 Hz and a characteristic-length ratio 0.5. The wind-shielding dome is thus a valid and advantageous apparatus for noise assessment of e.g. wind turbines, remaining compact in dimension. The dome allows a more accurate characterization of infrasonic emissions at higher mean wind speeds and/or stronger atmospheric turbulence degrees than would be possible with standard equipment.

The other tests and researches

Steven Cooper (Cooper, 2013)

The use of dB(A) for the assessment of large industrial wind turbines does not address low frequency noise (LFN) or infrasound due to the filter characteristics of the A-weighting curve. In seeking to address infrasound noise (typically identified as between 1Hz and 20Hz) some acousticians for the wind industry have used dB(G) and dB(Z) results. Both of these weighting curves exhibit significant roll offs in the frequency domain below 6Hz that renders the use of such descriptors of no real value in addressing infrasound of wind turbine noise. In my opinion the correct procedure is to use Linear (unweighted) levels in both constant percentage 1/3 octave bands (to agree with current acoustical data) and narrow band analysis to identify the wind turbine signature. For infrasound noise it would appear consideration of the linear result over the bandwidth of 1Hz – 20Hz is appropriate and low frequency noise when considered as a separate exercise should be expressed as a linear level restricted to the bandwidth of 20 – 200Hz. The concept of utilising dB(G) to describe infrasound levels associated with wind turbines at residential receivers has a fundamental flaw due to the definition of the G weighting curve which can be obtained by reference back to International Standard ISO 7196:1995. Due to the specific frequency weighting characteristics of the G function, whilst the proportion of energy below 6.3Hz is evident in a linear format for such measurements, such energy is not reflected in the dB(G) value. The relevance of using dB(G) to determine the human perception of infrasound from turbines has not been established or whether in fact the suggestion of a hearing threshold based on dB(G) is appropriate for turbine noise. There is danger in utilising or presenting material as Linear levels when using instrumentation that has a dB(Z) weighting. The filter of the Z curve rolls off in the infrasound region and does not provide Linear results that for persons not familiar with such issues lead to errors. Not all meters have the same dB(Z) filter or even true Linear spectrum results, nor do most consultants or calibration facilities have the ability to calibrate complete systems across the full infrasound spectrum. It would therefore appear that in seeking to investigate infrasound measurements the appropriate method is to present the linear (unweighted) results. In our experience in addition to generalised 1/3 octave band information, narrowband analysis should be provided which by its very nature is able to identify the presence of tones at a lower level than one can see by use of 1/3 octave band analysis. Investigations into the infrasound issue associated with the wind turbines also require consideration of the noise levels inside buildings. In some cases the internal noise levels are higher than external, whilst for other sites the internal levels are marginally below that recorded externally – but not to the extent as the reduction in dB(A) values. Apart from the issue of secondary windscreens or microphones in holes in the ground, there is an issue in terms of the instrumentation that is used for measurements where matters have been raised by various parties as to the noise floor of the microphone (and the instrumentation) and also the frequency response for the levels being measured. The frequency response of microphones is usually tested at levels much higher than encountered inside residences. Testing in our anechoic room showed the frequency response is not linear across the dynamic range [18] and one has to ensure the system can measure the actual noise – hence requiring specialised instrumentation. Investigation and measurement of infrasound is for most acousticians a new area of investigation and as well as being somewhat expensive to investigate, it is also quite interesting. It is hoped that the above matters lead to further discussion as to the appropriate measurements and consistency in terms of methodologies so as to permit the health studies and similar that would enable investigating noise from wind turbines can be undertaken from a more solid and consistent basis with respect to the noise level measurements.

Bruce Walker (Walker, 2013)

Measurement of infrasound radiation and reception from large wind turbines has been achieved with good success, with results that confirm the need to examine more than the power spectrum or L_{Geq} to evaluate potential human response. Emitted periodic waves appear to be characterized by a relatively steep wave-slope and moderately high crest factor. The amplitudes of observed wave harmonics appear to be well below known sensation thresholds. The author's conjecture is that perhaps the periodic sequence of relatively sharp time derivatives of pressure may in some individuals circumvent the evolved rejection of naturally occurring infrasound. Reporting of low-pass filtered, un-weighted sound pressure levels as turbine infrasound has been shown to exaggerate the magnitude of the issue by 10 dB or (much) more if microphones adequate to accurately record turbine emissions are employed. A portable measurement system comprising three low-frequency microphones, a turbine tachometer and dedicated time-domain signal analysis has been used to collect and evaluate infrasound emissions from large wind turbines. Field measurements of a 2-3 MW range turbine taken with this system indicate that acoustic energy at frequencies below the turbine blade passage rate is unrelated or weakly related to turbine operation. "Thump" waveforms produced by turbines were shown to be asymmetric and dependent on relative measurement and wind directions. At 100 meters, peak-to-peak amplitude is on the order of 0.5 Pa and peak rate of change of pressure is on the order 7 Pa/second. The data acquisition portions of the system were deployed in late 2012 on a field test to investigate indoor/outdoor infrasound levels at three homes abandoned by residents objecting to the location of eight 2.5 MW turbines within two km. At one residence, located approximately 400 meters from a turbine, outdoor to indoor coherence was observed for blade-pass harmonics 1-10 (0.7 – 7 Hz), with peak-to-peak thump amplitude approximately 0.26 Pa. Overall sound pressure in the frequency range 0.1 - 10 Hz fluctuated up to ± 7 Pa.

Kaj Dam Madsen, Torben Holm Pedersen (Madsen, 2011)

Low frequency noise and infrasound from large wind turbines is still a major concern when discussing new wind farms. New results from the Danish project "Low Frequency Noise from Large Wind Turbines" [1] funded by the Danish Energy Authority, Dong Energy, Vattenfall AB Vindkraft, E.ON Vind Sverige AB, Vestas Wind Systems A/S and Siemens Wind Power A/S is presented. The study is based on new measurements on large wind turbines representative for the large wind turbines installed in Danish wind farms during the last two years. An evaluation of the development in low frequency noise when comparing to older small turbines is made and differences are discussed. Methods for evaluation of the low frequency noise impact at residences close to wind turbines are presented. This includes all steps from measurement of noise characteristics of the wind turbines to the calculation of resulting indoor noise levels at nearby residences. Based on new measurement results from large wind turbines it is concluded that large wind turbines do not cause a special problem regarding impact of low frequency noise at residences close to wind turbines. It is seen that it is important to evaluate each project individually based on the specific data for the project with respect to wind turbine noise data, distances and terrain. A method for assessment of low frequency noise levels indoor at nearby residences is presented and demonstrated. The method has already been used for specific projects to provide a better and more precise basis for the debate on noise impact caused by these specific wind farms.

3. Law regulation in assessments of infrasound and low frequency WTN

Possible tonal issues associated with wind turbines are addressed in a number of the governing jurisdictions. This included several in Europe (Denmark, Germany, Sweden, and the United Kingdom), South Australia and two in the USA (Township of Jefferson and Shawano County). The tonal analysis is identical within all but one of these jurisdictions, which incorporated a 5 dB penalty added to the established threshold limits. Germany is the exception. It does include a penalty for possible tonal noise, but the penalty is 3 or 6 dB depending on the distinctiveness. Out of these jurisdictions, Shawano County is the only one that included a low frequency one-third octave band analysis. Denmark regulations also include a low frequency analysis from 10 Hz to 160 Hz, but this is a single overall number for this frequency range (Fowler, 2013).

Shawano Country Ordinance (USA)

Shawano County Ordinance (USA) regulates wind turbine noise by taking into account background noise levels at the property line of any non-participating property owner (Shawano County, no date). Noise associated with wind farms cannot exceed 5 dB(A) above the background noise levels for more than 5 minutes out of any one-hour time period at these property lines.

The County Ordinance also states that no low frequency noise or infrasound noise from wind turbine operations shall be created which causes the noise level both within the project boundary and a one-mile radius beyond the project boundary to exceed the limits provided in Table 9 below.

Table 1. Shawano Country (USA) One-Third Octave Band Noise Threshold Limits

1/3 Octave Band Center Frequency (Hz)	Sound Pressure Level (dB)
2 to 1	70 (each band)
16	68
20	68
25	67
31.5	65
40	62
50	60
63	57
80	55
100	52
125	50
250	47
500	45
1000	42
2000	40
4000	37
8000	35

Wind turbines that emit impulsive sound below 20 Hz that adversely affects the habitability or use of any existing dwelling unit, hospital, school, library, nursing home, or other sensitive noise receptor are considered unsafe and must be shut down immediately.

Denmark

Denmark has specific legislation on noise from wind turbines. In 2011 the existing statutory order on noise from wind turbines was revised to include limit values for low frequency noise (*Bekendtgørelse om støj fra vindmøller*, 2011). The new legislation entered into force on January 1st, 2012.

The noise parameters used are:

- the noise exposure level L_r for the total noise;
- the noise level L_{pALF} for the A-weighted low frequency noise in dwellings in the frequency range from 10 to 160 Hz.

The L_r -level includes a supplement of 5 dB(A) if the noise contains clearly audible tones.

The limit values for the noise exposure level L_r are:

- At dwellings in residential areas, holiday homes, etc.
 - 37 dB(A) at a wind speed of 6 m/s.
 - 39 dB(A) at a wind speed of 8 m/s.
- At dwellings in rural areas
 - 42 dB(A) at a wind speed of 6 m/s.
 - 44 dB(A) at a wind speed of 8 m/s.

The limit value for low frequency noise L_{pALF} is 20 dB at a wind speed of 6 and 8 m/s indoors in dwellings in both residential areas and rural areas.

In addition to the above mentioned noise limits, a setback distance of 4 times the total height of the wind turbine to dwellings has to be respected (*Cirkulære om planlægning for og landzonetilladelse til opstilling af vindmøller*, 2009).

4. Infrasonds' impact on human health

There is a lot of evidence that the environment and lifestyle can have a profound impact on mental health, and even on the morphology of the brain, and it obvious that Infrasound is ubiquitous in our lives today. The most common sources of infrasound are: traffic, large ventilation systems, public transport, wind farms, heat pumps and large machines (Leventhall, Pelmear and Benton, 2003).

Most of the reviews of studies on the analysis of the impact of infrasound on health were uncontrolled in the clinical sense. It was based on data related to industrial workers or observations of areas exposed to infrasound due to proximity to sources (Leventhall, 2007; Bolin *et al.*, 2011; Persinger, 2014). Such research is usually burdened with high ambiguity. For example, low-frequency audible components usually occurred during the exposure, which precluded an unambiguous answer to the question whether the adverse effects can be attributed only to infrasound or audible bands. Accordingly, the most recent reviews of studies on the influence of infrasound on human health adopt conservatism in concluding about the adverse health effects directly caused by infrasound. Psychological and social mechanisms have been suggested to contribute to annoyance, which explains the observed adverse health effects better than exposure to very low frequency noise (van Kamp and van den Berg, 2018). According to another report, about 10 percent of people living near infrasonic sources report general annoyance (Baliatsas *et al.*, 2016).

Most of previously cited reports usually highlight potential side effects such as nausea, malaise, fatigue, undefined pain, sleep disturbance, or irritability. However, there are also reports (Yount *et al.*, 2004; Vahl *et al.*, 2021) signaling the potential use of infrasound in oncological therapy as a supportive to the treatment with positive effects. A special case of infrasound may also be the phenomenon of binaural beats, which can be used in relaxation and sleep therapies (Kasprzak, 2014; Gálvez *et al.*, 2018), and the cited studies additionally indicate changes in the EEG (Electroencephalography) signal identical to exposure to infrasound.

Despite these strong indications regarding the effects of infrasound on mental health and cognitive functions in humans, there are virtually no studies that directly investigate infrasound effects on human health in a randomized and controlled manner. In addition, so far there are no studies analyzing the effect of infrasound on brain structure beside of work (Ascone *et al.*, 2021) in which the effect of long-term human exposure to infrasound compared to placebo was analyzed in a randomized manner. The presented study proved that long-term exposure (1 month) of infrasound with an amplitude above the values observed in wind farms and with a frequency of 6 Hz does not affect human behavior, including a number of variables related to health and psyche (i.e. self-assessment of sound sensitivity, sleep quality, psychosomatic symptoms or tension) and cognitive functions (i.e. alertness, constant attention, cognitive flexibility, divisive attention, attention shift, inhibition). At the same time, it has been observed that exposure to infrasound is associated with a decrease in gray matter in areas of the brain that are associated with somatomotor and cognitive functions, such as working memory (bilateral VIIIa cerebellum) and higher auditory processing (angular gyrus, BA39), including functions such as speech intelligibility / production or semantic / lexical processing and reading. In another study on the influence of infrasound directly on the brain (Dommes *et al.*, 2009) it was noted that exposure to infrasound caused a change in the BOLD (The Blood-Oxygen-Level-Dependent) signal in the primary auditory cortex and superior temporal gyrus. These are areas in the brain that are largely responsible for higher order auditory processing, such as language comprehension. Signal variations were seen at SPL levels between 90 and 110 dB for infrasound and low frequencies between 12 and 500 Hz.

5. Models of infrasounds

At the beginning of the development of modern wind turbines in the late 1970s, many different rotor concepts were considered and studied. Among them were twin-blade turbines with a downwind rotor, as well as three-blade turbines with an upwind rotor. Structurally, downwind turbines have a number of advantages compared to upwind turbines (Madsen *et al.*, 2007). On the other hand, one of the main disadvantages of the downwind rotor is the significant generation of low-frequency noise, usually in the range of 20 - 100 Hz, which may irritate local residents and people far away from the turbine. Generating low-frequency noise is related to the passage of the rotor blade near the tower, regardless of whether it is tubular or latticed. An additional feature of low-frequency noise is the fact that it changes significantly over time. The change in the amplitude of the measurement signal, even above 10 dB, is noted (Madsen *et al.*, 2007).

Currently, for low-frequency noise, calculations are most often performed in a sequential manner using the Computational Fluid Dynamics (CFD) model, the aeroelastic HAWC model and the acoustic model. The output data from the CFD model in the form of time courses of the components of the air stream velocity behind the tower (Figure 8) constitute the input data for the HAWC model. On the other hand, the output data from the HAWC model in the form of Fourier coefficients of the waveforms of the thrust and rotor torque are used as input data for the acoustic model. Madsen et

al. in (Madsen *et al.*, 2007) analyzed the influence of the jet instability behind the tower on the calculated values of low-frequency noise. The results presented by the authors (Figure 9) indicate an increase in the sound pressure level by 5-20 dB due to the instability of the stream caused mainly by the formation of vortices behind the turbine tower. At some time intervals, the sound pressure level may increase further from 0 to 10 dB as the rotor blades pass directly through the vortices behind the tower. The calculation results presented by the authors are consistent with the results of measurements of the sound pressure level around the turbines, which show large fluctuations due to stream instability, as well as a significant increase in the sound pressure level, if the frequency of the rotor blades passing is close to the frequency of vortex generation by the tower, which may be determined on the basis of the Strouhal number for the tower.

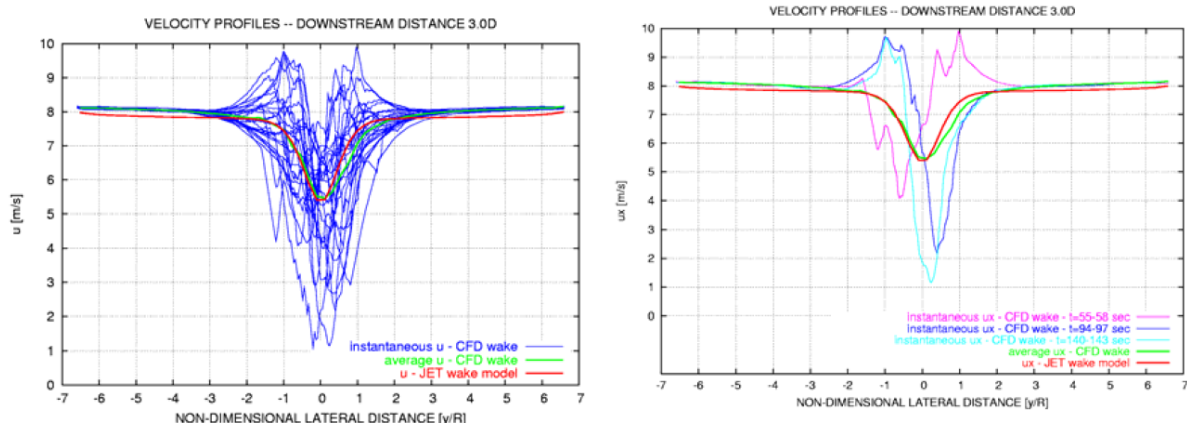


Figure 8. Stream velocity profile at a distance of 3D from the center of the tower, where D is the diameter of the tower (Madsen *et al.*, 2007)

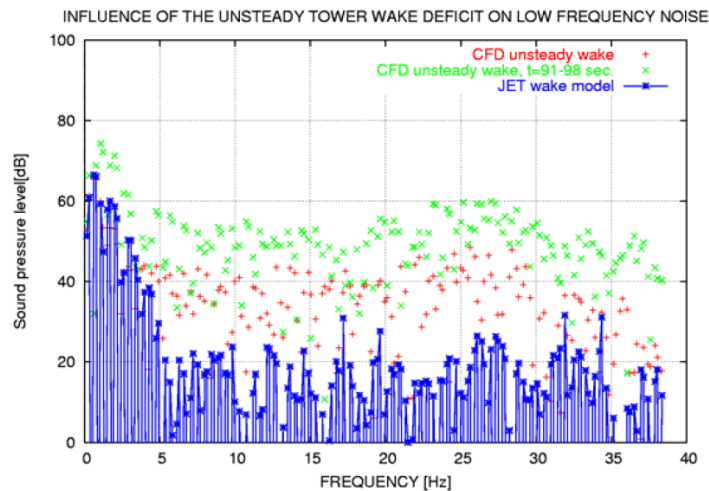


Figure 9. The calculated sound pressure level at a distance of 200 m behind the rotor, showing a strong influence of the non-stationary stream flow on low-frequency noise (Madsen *et al.*, 2007)

Madsen in work (Madsen, 2010) of 2010, based on numerical calculations using the same model as in (Madsen *et al.*, 2007), analyzed the influence of various design and operational parameters of the turbine on the level of low-frequency noise (LFN) at a distance of 400 m behind the turbine. The following parameters were analyzed:

- rotor type - upwind and downwind rotors,

- distance of the rotor from the tower,
- distance of the receiver point from the turbine tower,
- wind speed,
- speed of the blade tip,
- tower drag coefficient,
- tower diameter.

First, the author analyzed the impact of the rotor design, namely the positioning of the rotor blades in relation to the wind direction. In this respect, we can divide turbines with upwind or downwind rotors (Figure 10).

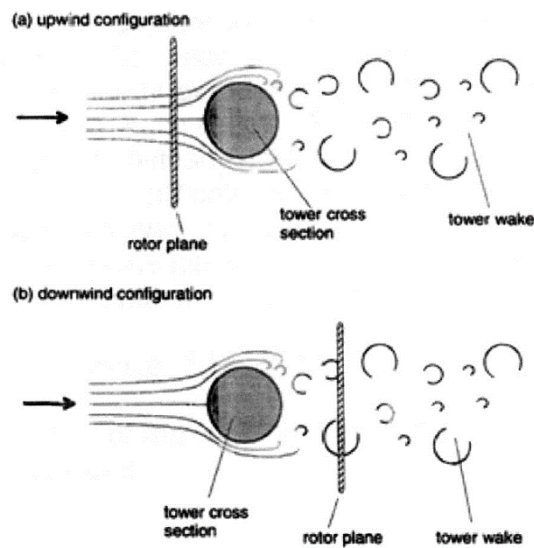


Figure 10. Types of wind turbines (Madsen, 2010)

The conducted analyzes showed that the downwind turbine generates 20 dB higher low-frequency noise level than the upwind turbine at different distances between the rotor and the tower (Madsen *et al.*, 2007). Based on the results (Figure 11), the author concluded that turbines operating with the rotor against the wind should not be a problem in terms of low-frequency noise emission to the environment (Madsen, 2010). On the other hand, increasing the distance between the blades and the tower by 1 m will reduce low-frequency noise by 2.8 dB.

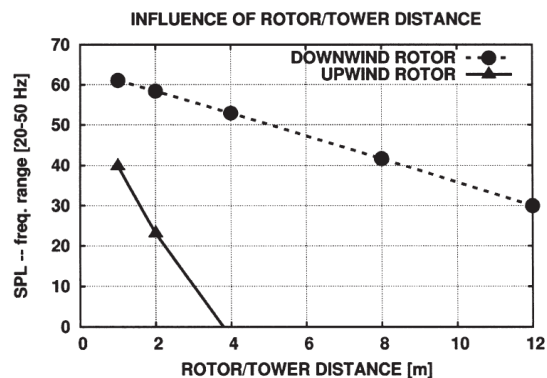


Figure 11. The total sound pressure level in the 20-50 Hz frequency band for upwind and downwind turbines as a function of the blade distance from the tower (Madsen, 2010)

Therefore, further analyzes have only been performed with the downwind rotor which generates higher levels of low frequency noise. The reason for this is that the vortices formed behind the tower are cut by the rotating blades of the rotor. This source of increased levels of low-frequency noise was also indicated in the publication (Madsen *et al.*, 2007). It has also been shown that an increase in the speed of the blade tip by 1 m/s causes an increase in the level of low-frequency noise by 0.8 dB (Madsen, 2010), while an increase in the tower drag coefficient causes a slight increase in LFN. The author also showed that with the increase of the tower diameter, the LFN level behind the turbine decreases, which is a result of a greater impact on the LFN level of the blade lift gradient as a function of time than the depth of the deficit of the wind speed behind the tower (Madsen, 2010).

Keith et al. (Keith, Daigle and Stinson, 2018) conducted a comparative analysis of the results of sound pressure level (SPL) modeling for infrasound and low-frequency sounds. The results of the calculations obtained using the parabolic equation (PE) method for the frequency of 0.5 Hz and the Fast Field Program (FFP) method for frequencies of 1.6 Hz and higher were compared with the calculation results obtained using the ISO 9613-2 method for the extended frequency range (below 63 Hz). These results were also compared with the results of long-term measurements conducted in Canada as part of the project: "Health Canada's Community Noise and Health Study".

The authors in (Keith, Daigle and Stinson, 2018) clearly showed that the harmonics related to the operation of the turbine are clearly visible in the signal spectrum even at a distance of 10 km from the turbine (Figure 12). They also emphasized that the measurement of infrasound from the turbine was largely influenced by ambient infrasound, the effectiveness of windbreaks and the presence of cover vegetation. The authors also found that the SPL from wind turbines is so low that effective windscreens should be used for infrasound measurements, and narrowband analysis should be used to distinguish turbine infrasonic noise from ambient noise, even in close proximity to the turbine. However, at wind speeds above 8 m/s, the measurement of infrasound generated by the turbine in accordance with IEC 61400-11 is very difficult or even impossible.

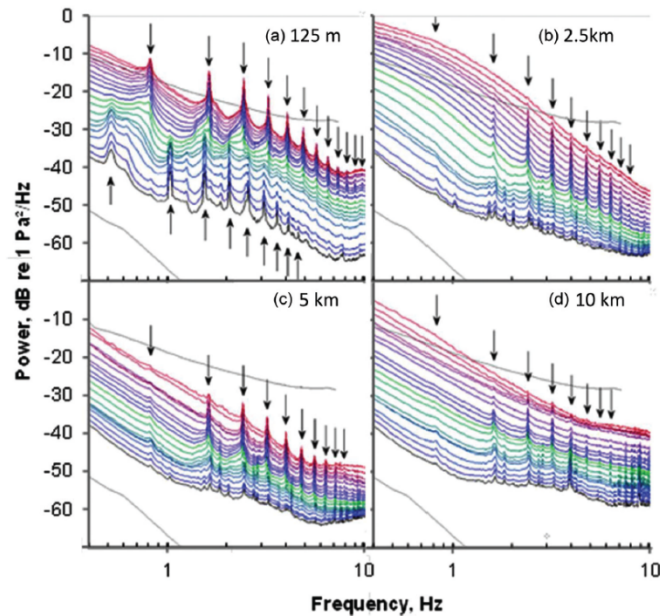


Figure 12. Spectrum of infrasound and low-frequency noise at various distances from the turbine (Keith, Daigle and Stinson, 2018)

The authors used two types of meteorological data in the calculations. These were weather classes according to Harmonoise, as well as actual measurement data extrapolated to a height of 1 km using the theory of similarity.

For the meteorological conditions described by the weather class W3S5 (strong inversion) in the frequency range below 5 Hz, the measurement results are consistent with the results of the downwind calculations. In the range from 5 to 20 Hz, the ambient noise has an influence on the measurement results within 10 km, while the ambient noise at 70 Hz has an influence on the results at any distance. Calculations of SPL using FFP based on meteorological data from measurements are closer to the measurement results than the results of calculations using weather classes compliant with Harmonoise (Figure 13). The difference between the results of the calculations obtained using the above-mentioned of the two types of meteorological data is usually 5 dB. However, the differences in the results of SPL measurements at a given measuring point do not exceed the value of 6 dB.

In conditions of low inversion occurring mostly on summer days (weather class according to Harmonoise W4S1), the noise of the wind turbines was measured with the wind at a distance of 2.5 and 5 km. The calculation results obtained with the use of both types of meteorological conditions were lower than the measurement results by at least 5 dB. At a distance of 10 km from the turbine, the calculation results between the analyzed types of meteorological data differ by almost 10 dB (Figure 14).

Wind turbine noise was also measured upwind during a weak daily inversion at wind speeds W4 (Figure 15). The results of calculations using the PE method with actual meteorological data were consistent with the measurement results. Due to the daytime inversion, which is not included in the Harmonoise weather classes, calculations are usually made for the W4 class. Then the results are usually underestimated.

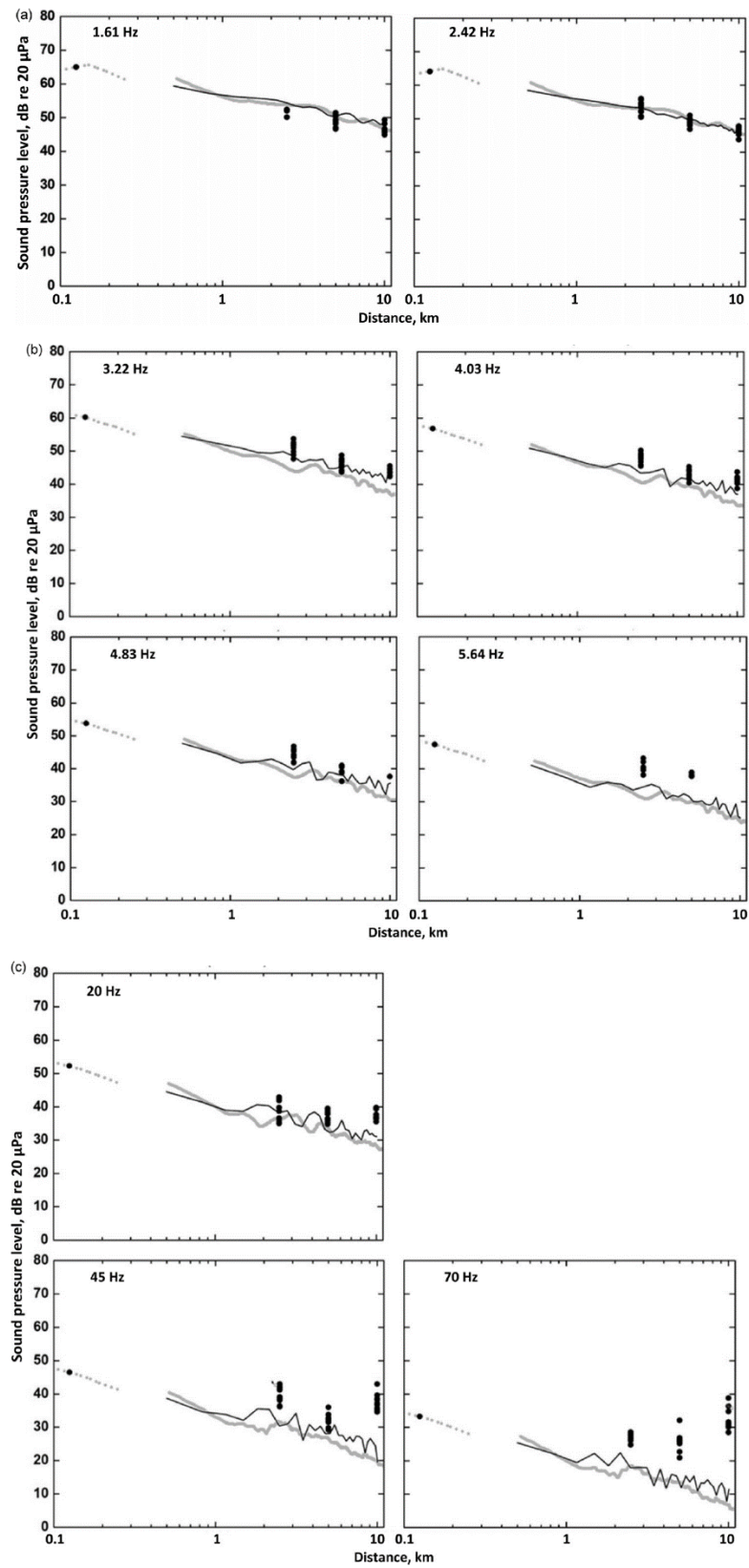


Figure 13. Comparison of calculated and measured SPL under high inversion conditions during an early summer morning as a function of distance from the turbine for selected frequencies. The measurement results are marked with black dots. The results of the FFP calculations using the actual meteorological data (wind speed 5 m/s at 10 m height, temperature

1.4 °C, 40° off from downwind) are marked with a thin black line, while the results of calculations using the Harmonoise W3S5 weather class are marked with a thick gray line (Keith, Daigle and Stinson, 2018)

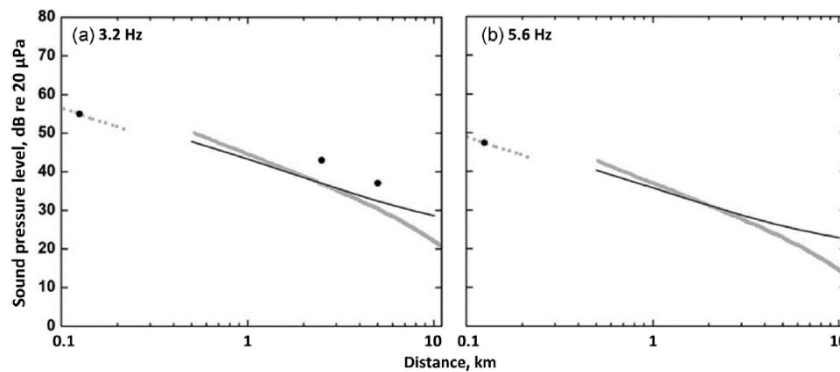


Figure 14. Comparison of calculated and measured SPL under low inversion conditions during a summer afternoon as a function of distance from the turbine for selected frequencies. The measurement results are marked with black circles. The results of the FFP method calculations using the actual meteorological data (wind speed 8.4 m/s at 10 m height, temperature -0.5 °C, 15° off from downwind) are marked with a thin black line, while the results of calculations using the Harmonoise W4S1 weather class are marked in gray thick line (Keith, Daigle and Stinson, 2018)

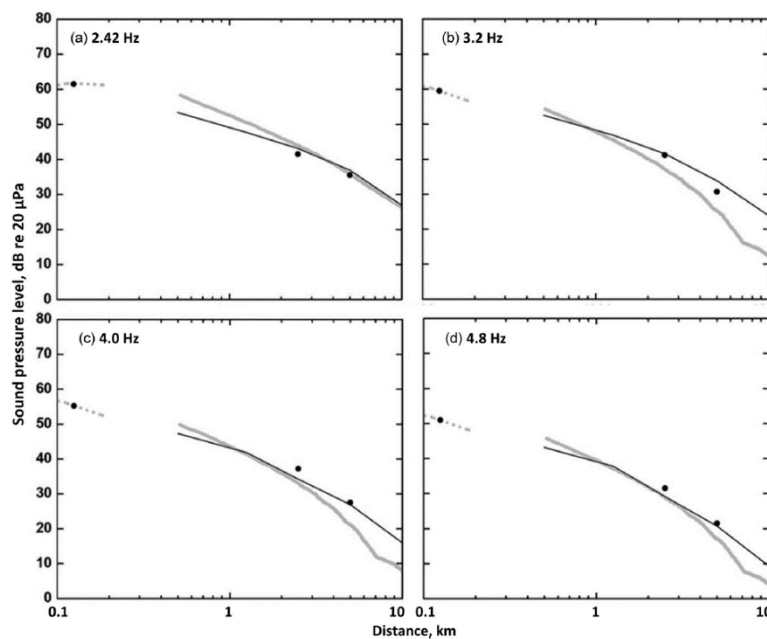


Figure 15. Comparison of calculated and measured SPL under low inversion conditions during early summer afternoon as a function of distance from the turbine for selected frequencies. The measurement results are marked with black circles. The results of the PE calculations using the actual meteorological data (wind speed 7 m/s at 10 m height, temperature 0.5 °C, 125° off from downwind) are marked with a thin black line, while the results of calculations using the Harmonoise W4S3 weather class are marked with a thick gray line (Keith, Daigle and Stinson, 2018)

As shown above, the sound velocity profiles obtained from actual meteorological data can represent conditions that are not included in the Harmonoise weather classes. Figure 16 shows the results of the SPL calculations for actual meteorological conditions indicating a weak temperature inversion, while the Harmonoise weather class indicated refracted rays. In this case, the SPL calculations using the Harmonoise class and actual meteorological conditions were similar at a distance of several hundred meters from the turbine, while at a distance of 10 km they differed by over 20 dB (Keith, Daigle and Stinson, 2018). The authors also found that calculations using the

Harmonise weather classes for long distances can result in serious errors and recommend the use of actual meteorological profiles.

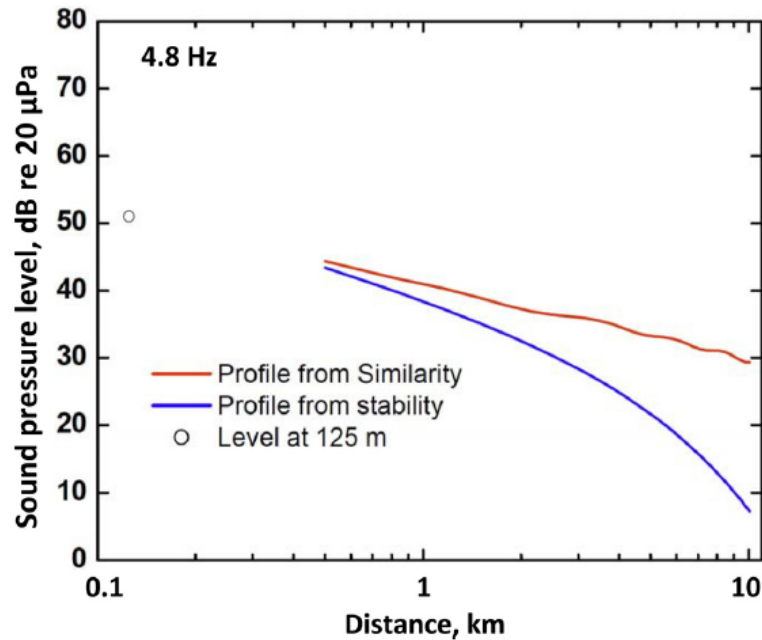


Figure 16. Comparison of the calculated SPL for the frequency of 4.8 Hz using the actual meteorological conditions (upper curve: wind speed 2 m/s at 10 m height, 0.3 °C temperature inversion measured between 2 and 10 m height, 35° off from downwind) with the values of the calculated SPL using the Harmonise weather class, which was determined on the basis of data from a nearby meteorological station (lower curve: W2S1, 5° off from downwind) (Keith, Daigle and Stinson, 2018)

Figure 17 shows a comparison of the annual average SPL calculated with the use of FFP using the Harmonise weather class and the ISO 9613-2 method in the extended frequency range. Correlation between the results obtained from the above-mentioned methods is very strong ($r \geq 0.9$). The compliance is better for lower SPL values, i.e. longer distances (Keith, Daigle and Stinson, 2018).

The authors conclude that the ISO 9613-2 calculation method with an extended frequency range can be used to calculate the annual average SPL of infrasound and low frequency noise when the assessed area is within a few kilometers from the nearest wind turbines. When calculations have to be made for large distances from the turbine or for specific meteorological classes, the authors recommend the use of the FFP method using the actual properties of the atmosphere.

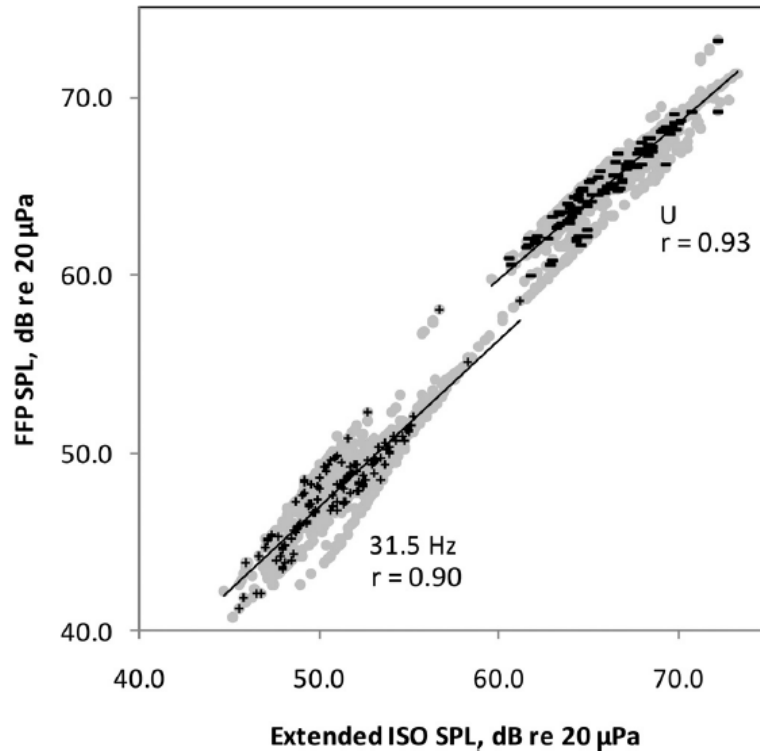


Figure 17. Comparison of the calculated SPL values in residential areas at a wind speed of 8 m/s using the FFP method and ISO 9613-2 with an extended frequency range. Data for the 31.5 Hz band are marked in the figure with the + symbol, while unweighted SPL values calculated for the frequency range from 0.5 Hz to 125 Hz with the symbol - values calculated for the frequency range from 0.5 Hz to 125 Hz with the symbol - (Keith, Daigle and Stinson, 2018)

In the work (Bertagnolio, Madsen and Fischer, 2017b) by Bertagnolio et al. analyzed the possibility of using the coupling of the HAWC2 aeroelastic model and the so-called Formula 1A developed by Farassat to model low-frequency noise generated by a wind turbine operating upwind.

HAWC2 is a multi-body aeroelastic model designed to simulate the loads on wind turbines. It is mainly used to predict structural loads and optimize power consumption. In this model, the Blade Element Momentum theory developed by Glauert is used to calculate the aerodynamic load resulting from the incoming wind and the rotation of the blades. In this model, unstable atmospheric features (e.g. turbulence, gusts) may also be taken into account, as well as other flow characteristics (e.g. trace of a windward turbine, disturbance of the flow around the tower) (Bertagnolio, Madsen and Fischer, 2017b). As a result of the implementation of this model, we obtain time courses of lift and aerodynamic drag, as well as the local angle of attack for each discrete blade element. This data is used in the next section as input to the LFN calculation.

Given the HAWC2 model outputs (angle of attack, lift, drag for each discrete airfoil element at each time step), the load vector can be determined. In the paper (Bertagnolio, Madsen and Fischer, 2017b), the authors used two load models. The first model, which they named M1, uses the Blade Element Momentum method, which does not require knowledge of the blade geometry as it treats the blade as a flat plate with a length equal to the blade chord (Fig. 11) at any given point in the blade span. The second model, called M2, uses the XFOIL algorithm, which allows to determine the lift and aerodynamic drag with the knowledge of the angle of attack for each element of the blade span (Figure 18).

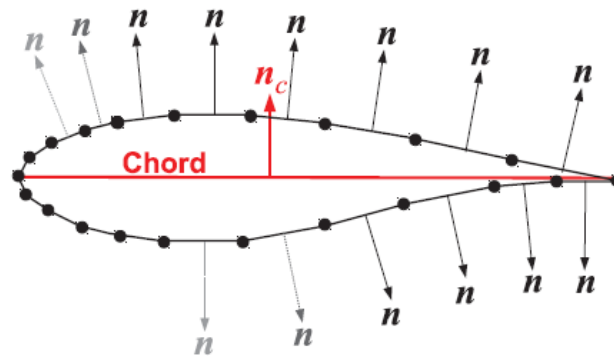


Figure 18. Blade geometry for load determination (Bertagnolio, Madsen and Fischer, 2017b)

The HAWC2 model has been extended to simulate the aeroacoustics of wind turbines by including additional models for turbulent inflow noise, trailing edge noise and stall noise. This extended model is known as HAWC2-Noise. This model calculates the spectrograms characteristic of the unstable aeroacoustic behavior of a wind turbine over time. In order to calculate the overall noise generated by a wind turbine, the obtained spectrograms should be averaged over time.

Formula 1A Farassat is a more elaborate expression of Ffowcs Williams-Hawkings. Its main advantage is that it gives relatively accurate calculations of the sound pressure generated by a surface or object moving in a fluid and its interaction with a variable aerodynamic load, as well as the sound pressure resulting from the fluid displacement produced by the thickness of the object itself.

In (Bertagnolio, Madsen and Fischer, 2017b), a model DTU 10MW wind turbine was modeled. It is a three-blade horizontal axis turbine with a rotor diameter of 178 m and a tower height of 119 m. The calculations assume a wind speed of 10 m/s at the height of the hub. At this wind speed, the rotational speed of the rotor is 8 rpm, which corresponds to a rotor rotation period of 7.5 s and a blade passage frequency of 0.4 Hz. The variability of wind speed as a function of height was described by the relation $V(h) = V_H (h/H)^{0.2}$, where h - height above the ground, H - height of the hub, V_H - wind speed at the height of the hub. LFN calculations were made for a distance of 205 m from the turbine, which is in line with the measurement point for this turbine for determining the sound power level of turbines according to IEC 61400 standards. All simulations were carried out within 300 s, of which the first 100 s were rejected to remove the initial transient effects from the analysis.

The authors in (Bertagnolio, Madsen and Fischer, 2017b) investigated the influence of various parameters on the LFN level at a point downstream of the turbine. The analysis was performed on:

- influence of Fourier transform time-windowing,
- influence of time-step,
- influence of loading model,
- influence of tower and wind shear,

- influence of inflow turbulence and disturbance caused by the operation of the preceding turbine.

The calculation results obtained from this model were also compared with other models used for wind turbine noise modeling, namely the Viterna's (Viterna, 1982)(Viterna, 1981) and Amiet's (Amiet, 1975) models.

First, the authors analyzed the effect of the size of the Welch time window used in the Fourier analysis to determine the sound pressure level. Two sizes of this window are used: small and large. Each of them gives a narrowband power spectrum, on the basis of which the sound pressure level is calculated.

Figure 19 shows the results of LFN modeling using the M1 load model for a turbine operating in a 100% disturbed field by the operation of the turbine located directly in front of the tested turbine with turbulence intensity at the level of $TI = 10\%$.

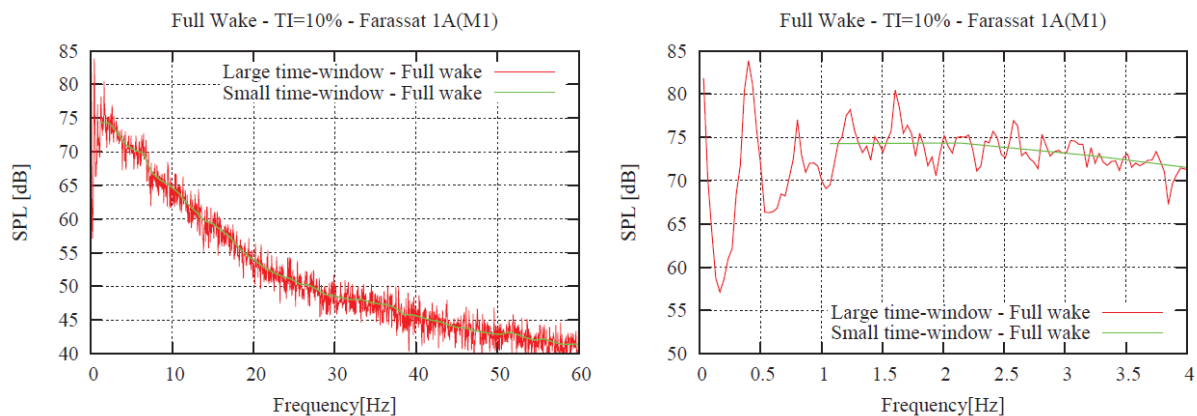


Figure 19. Spectrum of the sound pressure level - the effect of the size of the time window (Bertagnolio, Madsen and Fischer, 2017b)

The graph on the left side shows the spectrum in the frequency range up to 60 Hz, while the right side shows an approximate fragment of this spectrum up to 4 Hz. When a large window is used, numerous peaks in the spectrum are visible, which are averaged when a small time window is used. The spectrum obtained with the use of a large time window shows a peak related to the frequency of the blade's passage through the tower, which is 0.4 Hz, and its harmonics (0.8, 1.2 and 1.6 Hz). Above the latter frequency, the harmonics are less visible because they are most likely dominated by the turbulence noise of the inflow, which is characterized by broadband spectral energy as a result of the chaotic nature of the noise-generating turbulence (Bertagnolio, Madsen and Fischer, 2017b). In subsequent analyzes, unless explicitly stated, the results obtained with the use of a small time window will be presented.

Next, the influence of the time step used in the HAWC2-Noise model was analyzed. Three time steps were tested: 3.65, 7.3, 14.6 ms in order to be able to present the spectrum to the frequencies 136, 68 and 34 Hz respectively. Figure 20 shows the results of LFN calculations using the M1 load model for a turbine operating in a 100% disturbed field by the operation of the turbine located directly in front of the tested turbine with turbulence intensity at the level of $TI = 10\%$. By analyzing

the spectra obtained with the use of various time steps, it can be clearly stated that the influence of the time step has a slight impact on the calculated sound pressure level, but only changes the maximum frequency to which the calculations can be performed. In the further part of the analyzes, unless it is explicitly indicated, a time step of 7.3 ms will be used in order to shorten the computation time (Bertagnolio, Madsen and Fischer, 2017b).

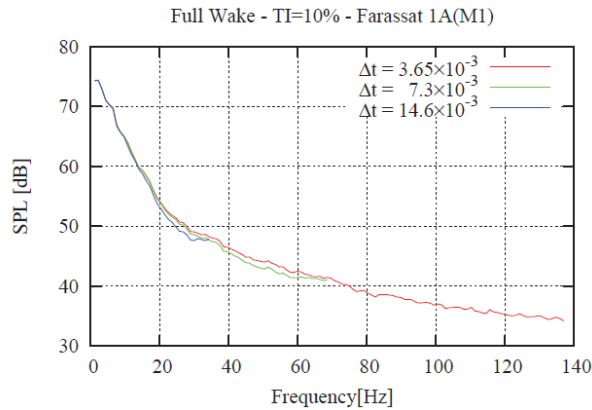


Figure 20. Spectrum of the sound pressure level - influence of the time step (Bertagnolio, Madsen and Fischer, 2017b)

Thirdly, the influence of the blade loading model on the results of LFN calculations was examined. Two models that are used in Farassat's Formula 1A were analyzed, namely the previously described M1 and M2 models. Figure 21 shows the modeling results for a turbine operating in an undisturbed field for two levels of atmospheric turbulence intensity $TI = 1\%$ and $TI = 10\%$.

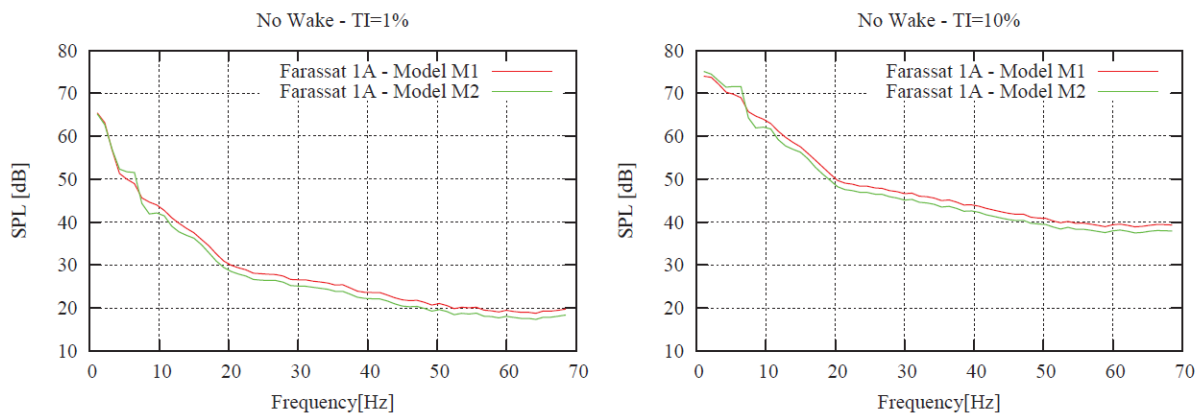


Figure 21. The spectrum of the sound pressure level - the influence of the load model (Bertagnolio, Madsen and Fischer, 2017b)

Both the M1 and M2 models give quite similar results for the sound pressure level, with the M1 model getting slightly higher results, from 1 to 2 dB, at frequencies higher than 7 Hz. However, for the frequency range up to 7 Hz, the obtained results are similar or higher for the M2 model (Bertagnolio, Madsen and Fischer, 2017b). In subsequent analyzes, unless explicitly indicated, the results obtained with the use of the M1 model will be presented due to the shorter computation time, which results from the use of the simplified blade geometry in this model.

The next stage of the analyzes was to determine the impact of disturbances caused by the tower and wind shear. The calculations were performed for the turbine operating in an undisturbed field

for the atmospheric turbulence intensity level $TI = 10\%$, the results of which are shown in Figure 22 for both the small and large time window. 4 different cases were analyzed:

- with a tower and wind shear,
- without a tower,
- no wind shear,
- without tower and wind shear.

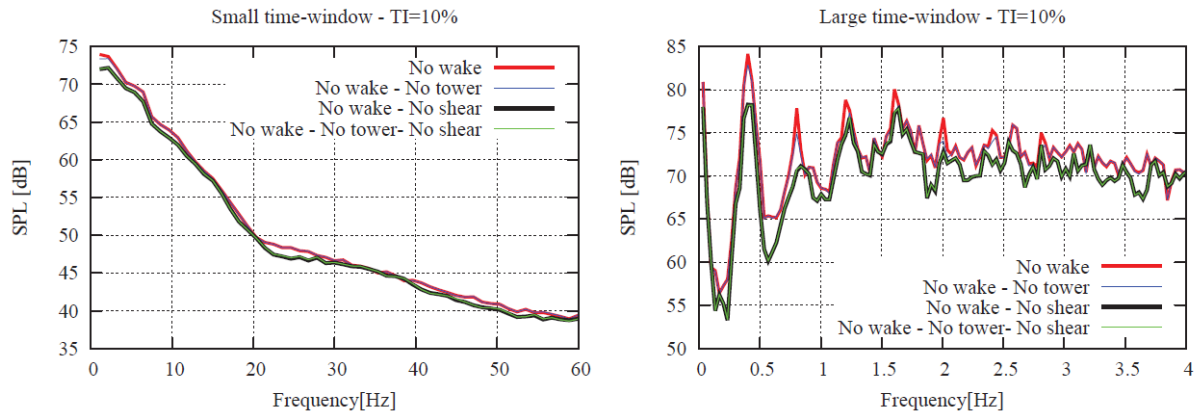


Figure 22. Spectrum of acoustic pressure level - influence of disturbances caused by the tower and wind shear (Bertagnolio, Madsen and Fischer, 2017b)

Figure 1. Spectrum of acoustic pressure level - influence of disturbances caused by the tower and wind shear (Bertagnolio, Madsen and Fischer, 2017b).

From the results shown in Figure 22, it seems that the tower has almost no influence on the calculated sound pressure level. However, it should be remembered that the analyzed turbine works against the wind. Whereas the effect of the tower will be more apparent when analyzing the LFN levels in the downwind turbine system, there will be a higher SPL level due to the significant flow deficit created by the tower footprint / shadow. On the other hand, wind shear slightly reduces the broadband part of the LFN and has a noticeable effect on the peak of the blade transition frequency (0.4 Hz) and its harmonics (Bertagnolio, Madsen and Fischer, 2017b).

The influence of inflow turbulence ($TI = 1\%$, $TI = 10\%$) and field disturbances caused by the turbine working in front of the tested turbine on the LFN level were also analyzed. The HAWC2 model enables the modeling of the effects of atmospheric turbulence using the Mann model to generate a 3D turbulent flow field. In addition, it also enables modeling the disturbance of the turbine field by the turbines working in front of the analyzed turbine using the Dynamic Wake Meandering model. In this analysis, it was assumed that the field disturbance is caused by the same turbine that works in front of the analyzed turbine at a distance of 3 rotor diameters, i.e. 535 m. Three disturbance configurations were analyzed. In the first, the wind turbine is located directly in front of the tested turbine and is marked as "full (100%) disturbance". Two configurations are then considered: the field disturbance by the operation of the upstream turbine may include disturbance meandering due to the convective effects of large-scale atmospheric turbulence, or no interaction. The third configuration is a case in which the preceding turbine is shifted in relation to the analyzed turbine by half of the rotor diameter perpendicular to the wind direction and it is marked as "half demolition" and always includes disturbance meandering (Bertagnolio, Madsen and Fischer, 2017b).

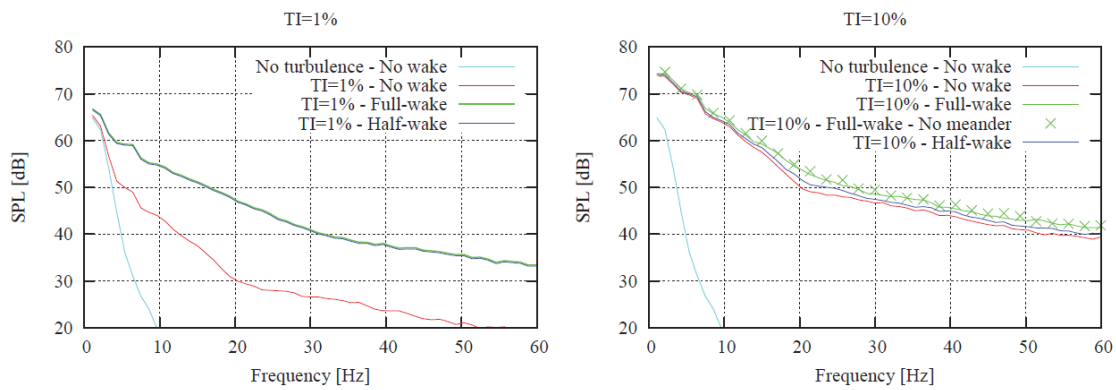


Figure 23. The spectrum of the acoustic pressure level - the influence of the inflow turbulence and disturbances caused by the operation of the preceding turbine (Bertagnolio, Madsen and Fischer, 2017b)

Figure 23 shows the calculation results also for the case in which neither the atmospheric turbulence nor the field disturbance caused by the operation of the preceding turbine were taken into account. For a higher level of atmospheric turbulence $TI = 10\%$, slight changes in the sound pressure level (in the range of 2 to 4 dB) are observed in the case of 100% field disturbance by the preceding turbine at a frequency of about 15 Hz. Slightly higher levels are also observed for the same configuration compared to "half perturbation". Switching off the meandering disturbance in the calculations using the HAWC2 model for 100% field disturbance has almost no effect on the SPL results (Bertagnolio, Madsen and Fischer, 2017b).

For the level of turbulence intensity $TI = 1\%$, the results indicate that the presence of 100% or a half field disturbance causes an increase in SPL even by approx. 16 dB compared to the case without field disturbance (Bertagnolio, Madsen and Fischer, 2017b).

The results were then compared with the Viterna's model used to calculate the LFN. Viterna developed a model based on the time series of the total load exerted on the rotor, namely the lift force and the torque (Viterna, 1982)(Viterna, 1981). In this case, the use of the HAWC2 model and Formula 1A leads to the determination of the same parameters as in the case of the Viterna's model, i.e. the lift force and torque time series.

The comparison of the results from both models for two levels of atmospheric turbulence and for several configurations is presented in Figure 24.

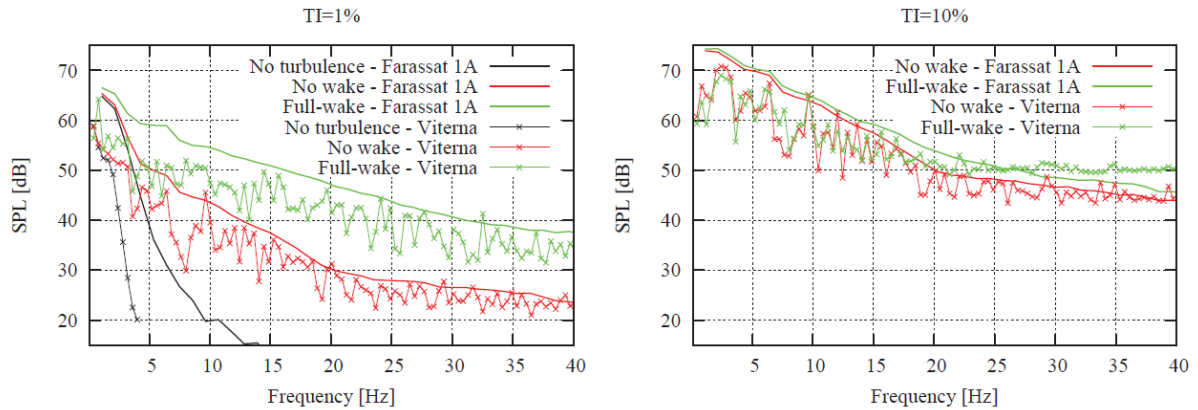


Figure 24. The spectrum of the sound pressure level - comparison with the Viterna's model (Bertagnolio, Madsen and Fischer, 2017b)

There is relatively good agreement between the two models. The Viterna's model exposes irregular SPL levels that appear as alternating peaks and lows. Nevertheless, the maximum values of these irregular peaks follow the general trends of the spectra calculated by Formula 1A. In the case of no turbulence, however, the results are very different. Overall, the Viterna's model appears to predict slightly lower sound pressure levels in the low frequency range, below say 10 to 15 Hz. It can be seen that for frequencies greater than 20 Hz, the Viterna's model predicts higher sound pressure levels than Formula 1A for a 100% perturbation configuration with TI = 10% turbulence, while the SPL levels agree when considering the no perturbation case. The reasons for this discrepancy have not yet been clarified (Bertagnolio, Madsen and Fischer, 2017b).

Then, the calculation results obtained from the HAWC2 model and Formula 1A were compared with the results obtained using the Amiet's model (Amiet, 1975), which is used to calculate the aerodynamic noise generated by the interaction of turbulent flow with the profile. This model has been implemented in the HAWC2-Noise algorithm (Bertagnolio, Madsen and Fischer, 2017b).

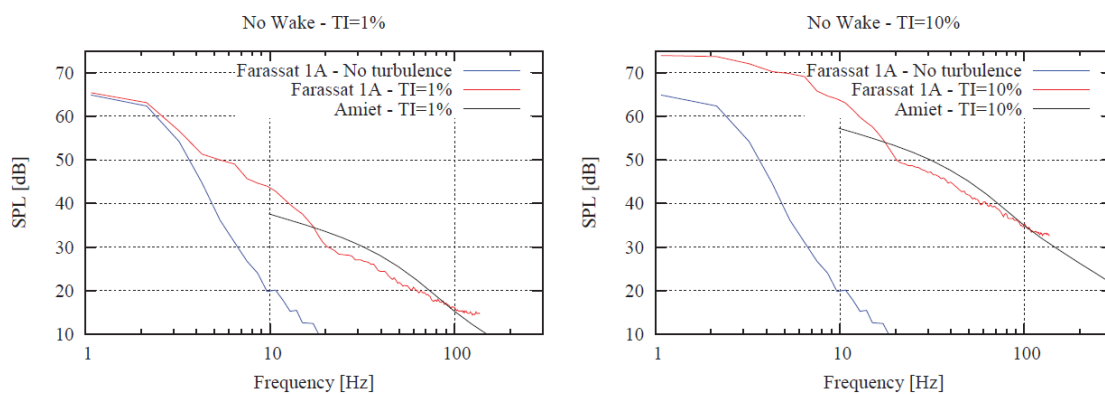


Figure 25. Spectrum of the acoustic pressure level - comparison with the Amiet's model (Bertagnolio, Madsen and Fischer, 2017b)

The results obtained from both models are presented in Figure 25 for two levels of turbulence intensity TI = 1% and TI = 10%, using the time step of 3.65 ms, which allows to perform calculations in the range up to 136 Hz (Bertagnolio, Madsen and Fischer, 2017b).

When analyzing the results presented in Figure 25, there is a relatively good agreement between the Amiet's spectral theory and the Fourier transform of the time simulations using Formula 1A for both turbulence intensities above 20 Hz. Although the difference in sound pressure level can be as high as 4 to 5 dB, the spectral slope of the two methods is almost the same above this frequency. Below 20 Hz Formula 1A shows a sudden change in slope from an almost linear slope above (on a log scale). This may suggest that below 20 Hz the Formula 1A-modeled sound source mechanism dominates and is not included in the Amiet's model. The effect of wind or tower shear did not explain this change in pitch. In summary, the discrepancies between Formula 1A and Amiet's theory for frequencies below 20 Hz can be due to the following reasons:

- not taking into account the larger scale turbulent structure in the Amiet's model, i.e. in the spectrum of Von Kármán used to describe the turbulent tributary,
- or alternatively that the scattering phenomenon for the compact airfoil is no longer actual (accounted for) in the Amiet's model at these low frequencies (Bertagnolio, Madsen and Fischer, 2017b).

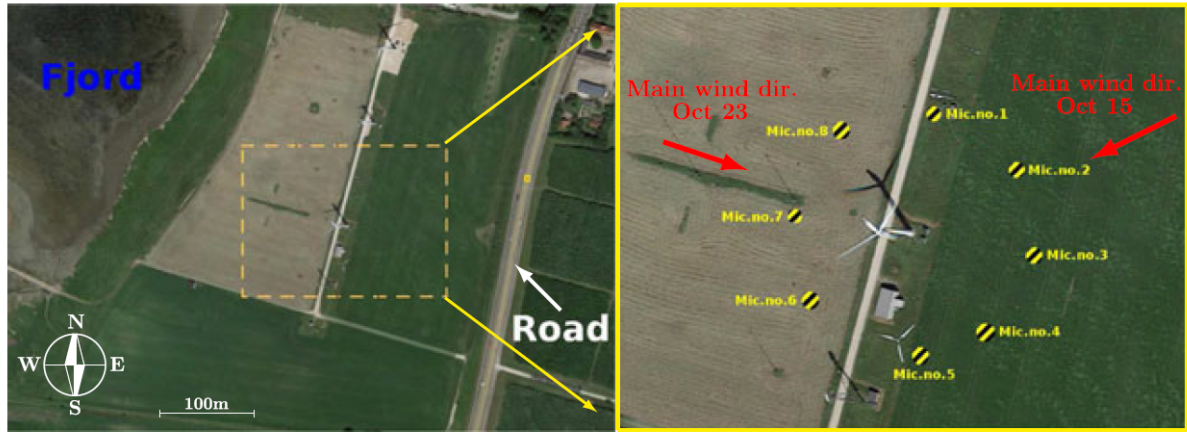
The Mann's model for atmospheric turbulence was also implemented in the Amiet's model as part of the HAWC2-Noise algorithm. It was verified that the use of this model instead of the Von Kármán spectrum did not change the above conclusions.

Above 20 Hz, the relatively good agreement between the Amiet's model and Formula 1A suggests that the turbulence noise has become the dominant sound source, and the Von Kármán spectrum is an acceptable approximation for atmospheric turbulence at these frequencies, at least for LFN generation.

The authors showed that the proposed calculation method gives results consistent with the existing other calculation methods. The main conclusion from these analyzes is the fact that the field disturbances caused by the preceding turbine have a significant impact on the LFN level generated by the tested turbine when the intensity of atmospheric turbulence is low. When the turbulence intensity is high, the influence of the field disturbance caused by the operation of the preceding turbine on the LFN level is low.

The proposed computational model in publication (Bertagnolio, Madsen and Fischer, 2017b) has been experimentally verified in (Bertagnolio, Madsen and Fischer, 2017a)(Franc, Aagaard and Andreas, 2019). The authors compared the results of numerical calculations with the results of measurements for two test wind turbines located at the DTU-Riso station. The first is the Nordtank NTK 500 turbine with a rotor diameter of 41 m and a hub height of 36 m, operating at a constant speed, while the second is the Vestas V52 with a rotor diameter of 52 m and a height of 44 m, operating with variable speed control.

Eight measuring microphones are placed around the turbine on plywood plates. The location of the measurement points around the NTK 500 turbine is shown in Figure 26.

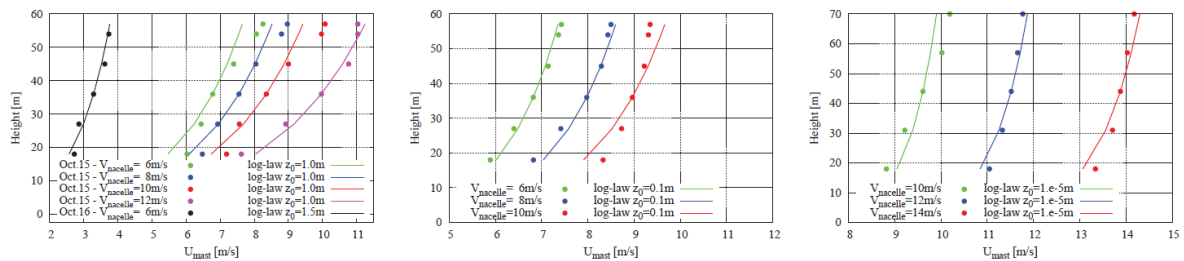


(a) Wide view including nearby road and fjord

(b) Close-up view with microphones distribution and main wind directions

Figure 26. Location of measurement points around the NTK 500 turbine (Bertagnolio, Madsen and Fischer, 2017a)

All input parameters to the Mann's model, i.e. wind shear and the intensity of atmospheric turbulence at the height of the hub, were determined on the basis of measurement data recorded at the measurement site. Due to the fact that they are test turbines, they were equipped with various sensors mounted on the tower and turbine hub, allowing to determine all the necessary input parameters for the model. There are also meteorological masts in the vicinity of these turbines, which monitor the weather conditions at various heights up to the "tip" of the wind turbines. The wind speed profiles recorded during the measurement sessions are shown in Figure 27.



(a) NTK turbine on Oct. 15 & 16 - $z_0 = 1.0$ & 1.5 m

(b) NTK turbine on Oct. 23 - $z_0 = 0.1$ m

(c) V52 turbine - $z_0 = 10^{-5}$ m

Figure 27. Wind speed profiles recorded during measurement sessions (Bertagnolio, Madsen and Fischer, 2017a)

Figure 28 presents the results of numerical calculations with the results of LFN measurements generated by the turbines, as well as with the results of the acoustic background measurement recorded around the turbines.

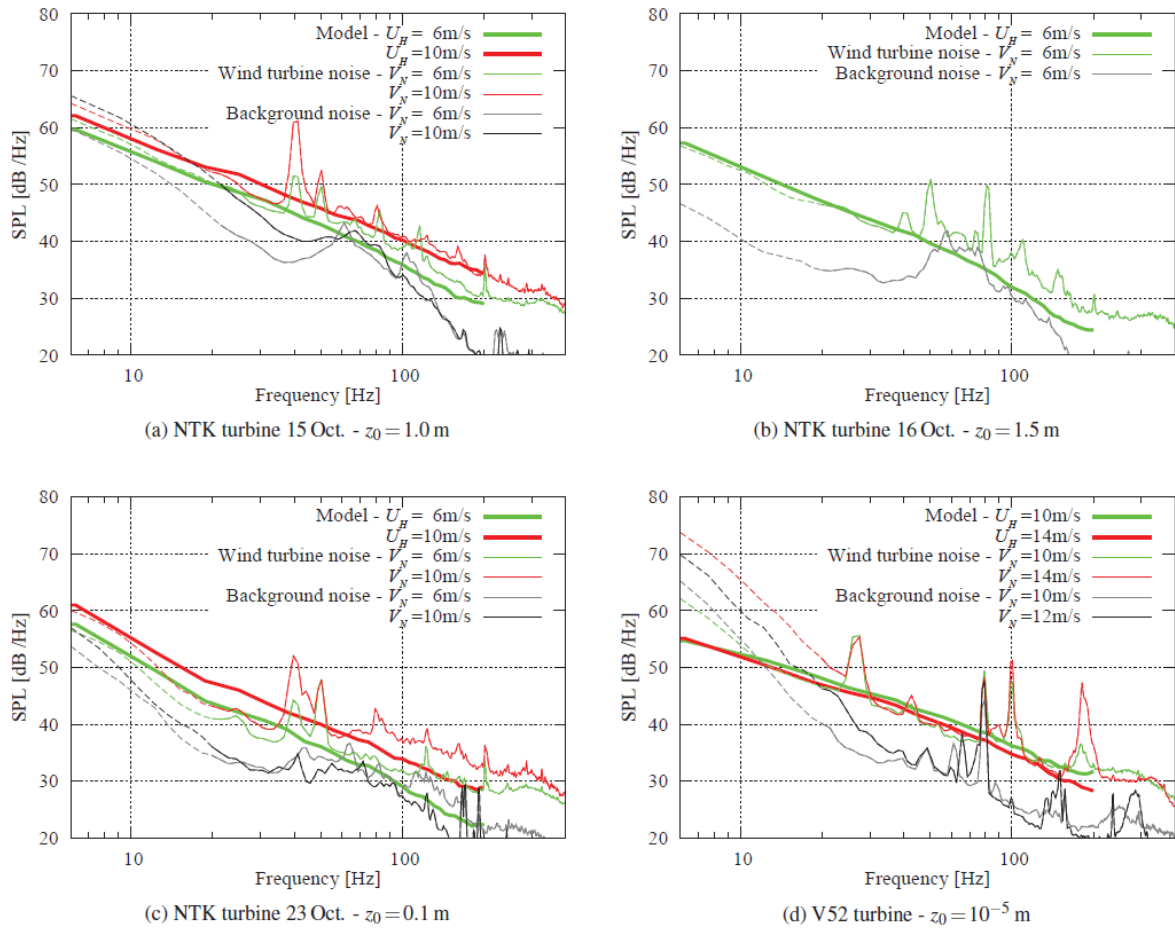


Figure 28. The spectrum of the caustic pressure level for NTK 500 and V52 turbines (Franc, Aagaard and Andreas, 2019). The results of model calculations are marked with a thick line. The measurement results are marked with a thin line. The dashed line shows the measurement results for frequencies below 20 Hz.

Figure 2. The spectrum of the caustic pressure level for NTK 500 and V52 turbines (Franc, Aagaard and Andreas, 2019). The results of model calculations are marked with a thick line. The measurement results are marked with a thin line. The dashed line shows the measurement results for frequencies below 20 Hz.

When analyzing the results presented in Figure 28, it can be noticed that the background noise disturbs the measurement results for the NTK 500 turbine in the frequency range from 40 to 100 Hz, mainly at low wind speeds (Figure 28b). Most likely, this disruption is due to nearby traffic and vegetation. In addition, the graphs show numerous "false" peaks, the source of which is the mechanical noise generated in the nacelle. The measurement results for the V52 turbine, which are shown in Figure 28d, also have such peaks in the same frequency range. The same peaks can also be seen in the acoustic background noise spectrum and most likely their source are devices inside the nacelle that operate even when the rotor is at a standstill, e.g. cooling fans (Franc, Aagaard and Andreas, 2019).

The measurement results are also distorted in the frequency range below 20 Hz, except in the case of October 16 for NTK 500. These disturbances most likely come from ambient and vegetation noise, which is less dominant in the measurements on October 16 due to the lower wind speed on that day (Franc, Aagaard and Andreas, 2019). Nevertheless, the measurement results agree with the calculation results below this frequency.

The authors found a good agreement of the measurement results with the calculation results, disregarding the background noise. The model results correctly reproduce the quantitative increase in LFN as a function of wind speed, although in some cases and in some frequency ranges the differences in relation to the measured data are visible (Franc, Aagaard and Andreas, 2019).

References

- Amiet, R. K. (1975) 'Acoustic radiation from an airfoil in a turbulent stream', *Journal of Sound and Vibration*, 41(4), pp. 407–420. doi: 10.1016/S0022-460X(75)80105-2.
- Ascone, L. *et al.* (2021) 'A longitudinal, randomized experimental pilot study to investigate the effects of airborne ultrasound on human mental health, cognition, and brain structure', *Scientific Reports*, 11(1), p. 5814. doi: 10.1038/s41598-021-83527-z.
- Baliatsas, C. *et al.* (2016) 'Health effects from low-frequency noise and infrasound in the general population: Is it time to listen? A systematic review of observational studies', *Science of The Total Environment*, 557–558, pp. 163–169. doi: 10.1016/j.scitotenv.2016.03.065.
- Bekendtgørelse om støj fra vindmøller* (2011). Denmark: Miljøministeriet.
- Bertagnolio, F., Madsen, H. A. and Fischer, A. (2017a) 'A combined aeroelastic-aeroacoustic model for wind turbine noise: verification and analysis of field measurements', *Wind Energy*, 20(8), pp. 1331–1348. doi: 10.1002/we.2096.
- Bertagnolio, F., Madsen, H. A. and Fischer, A. (2017b) 'A temporal wind turbine model for low-frequency noise', in *INTER-NOISE and NOISE-CON Congress and Conference Proceedings*. Hong Kong: Institute of Noise Control Engineering, pp. 5025–5033.
- Betke K, Schults von Glahn M and Goos O (1996) 'Messung der Infraschallabstrahlung von windkraftanlagen', *Proc DEWEK*, pp. 207–210.
- Bolin, K. *et al.* (2011) 'Infrasound and low frequency noise from wind turbines: Exposure and health effects', *Environmental Research Letters*, 6(3). doi: 10.1088/1748-9326/6/3/035103.
- Carman, R. A. (2015) 'Measurement procedure for wind turbine infrasound', *INTER-NOISE 2015 - 44th International Congress and Exposition on Noise Control Engineering*, (August).
- Cirkulære om planlægning for og landzonetilladelse til opstilling af vindmøller* (2009). Denmark: Miljøministeriet.
- Cooper, S. (2013) 'The Measurement of Infrasound and Low Frequency Noise for Wind Farms', *5th International Conference On Wind Turbine Noise Denver 28-30 August 2013*.
- D'Amico, S., Van Renterghem, T. and Botteldooren, D. (2021) 'Measuring infrasound outdoors with a focus on wind turbines: the benefits of a wind-shielding dome', *Applied Acoustics*, 178, p. 108015. doi: 10.1016/j.apacoust.2021.108015.
- DIN 45680 (1997) 'Measurement and Assessment of Low-Frequency Noise Immision in the Neighbourhood'.
- Dommes, E. *et al.* (2009) 'Auditory cortex stimulation by low-frequency tones—An fMRI study', *Brain Research*, 1304, pp. 129–137. doi: 10.1016/j.brainres.2009.09.089.
- Fowler, K. (2013) 'International Legislation and Regulations for Wind Turbine Noise', *5th International Conference on Wind Turbine Noise Denver 28–30 August 2013*.

- Franc, B., Aagaard, M. H. and Andreas, F. (2019) 'Analysis of low-frequency noise from wind turbines using a temporal noise code', in *Proceedings of the 23rd International Congress on Acoustics*. Deutsche Gesellschaft für Akustik, pp. 4414–4421.
- Gálvez, G. *et al.* (2018) 'Short-Term Effects of Binaural Beats on EEG Power, Functional Connectivity, Cognition, Gait and Anxiety in Parkinson's Disease', *International Journal of Neural Systems*, 28(05), p. 1750055. doi: 10.1142/S0129065717500551.
- Hansen, K. (2013) 'Evaluation of secondary windshield designs for outdoor measurement of low frequency noise and infrasound', *5th International Conference on Wind Turbine Noise Denver 28-30 August 2013*.
- Hayes McKenzie Partnership (2006) 'The Measurement of Low Frequency Noise at Three UK Wind Farms', *UK Department of Trade and Industry (DTI)*.
- Hu, W. (2018) *Advanced Wind Turbine Technology*, Springer. Springer.
- Hubbard, H. H. and Shepherd, K. P. (1990) 'Wind Turbine Acoustics', *NASA*.
- Hubbard, H. H. and Shepherd, K. P. (2009) 'Wind turbine acoustics', *NASA Langley Research Center*, pp. 153–183. doi: 10.2495/978-1-84564-205-1/05.
- ISO 7196:1995 (no date) 'Acoustics – Frequency weighting characteristics for infrasound measurements'.
- van Kamp, I. and van den Berg, F. (2018) 'Health Effects Related to Wind Turbine Sound, Including Low-Frequency Sound and Infrasound', *Acoustics Australia*, 46(1), pp. 31–57. doi: 10.1007/s40857-017-0115-6.
- Kasprzak, C. (2014) 'The influence of infrasounds on the Sensory Motor Rhythm (SMR) of EEG Signal', *Forum Acusticum 2014*.
- Keith, S. E., Daigle, G. A. and Stinson, M. R. (2018) 'Wind turbine low frequency and infrasound propagation and sound pressure level calculations at dwellings', *The Journal of the Acoustical Society of America*, 144(2), pp. 981–996. doi: 10.1121/1.5051331.
- Kłaczyński, M. and Wszótek, T. (2014) 'Acoustic study of REpower MM92 wind turbines during exploitation', *Archives of Acoustics*, 39(1), pp. 3–10. doi: 10.2478/aoa-2014-0001.
- Leventhall, G. (2007) 'What is infrasound?', *Progress in Biophysics and Molecular Biology*, 93(1–3), pp. 130–137. doi: 10.1016/j.pbiomolbio.2006.07.006.
- Leventhall, G., Pelmear, P. and Benton, S. (2003) 'A review of published research on low frequency noise and its effects', *Department for Environment, Food and Rural Affairs (DEFRA)*.
- Madsen, H. A. *et al.* (2007) 'Simulation of Low Frequency Noise from a Downwind Wind Turbine Rotor', in *45th AIAA Aerospace Sciences Meeting and Exhibit*. Reston, Virginia: American Institute of Aeronautics and Astronautics. doi: 10.2514/6.2007-623.
- Madsen, H. A. (2010) 'Low Frequency Noise from Wind Turbines Mechanisms of Generation and its Modelling', *Journal of Low Frequency Noise, Vibration and Active Control*, 29(4), pp. 239–251. doi: 10.1260/0263-0923.29.4.239.
- Madsen, K. D. (2011) 'Noise from large wind turbines – an update on low frequency noise', *Fourth International Meeting on Wind Turbine Noise, Rome Italy 12-14 April 2011*.

O'Neal, R., Hellweg, R. D. J. and Lampeter, R. (2009) 'A Study of Low Frequency Noise and Infrasound from Wind Turbines', *Epsilon Associates Inc, Maynard*.

Pantazopoulou, P. (2009) 'Wind turbine noise measurements and abatement methods', *WIT Transactions on State of the Art in Science and Engineering*, 34, pp. 641–659. doi: 10.2495/978-1-84564.

Persinger, M. A. (2014) 'Infrasound, human health, and adaptation: an integrative overview of recondite hazards in a complex environment', *Natural Hazards*, 70(1), pp. 501–525. doi: 10.1007/s11069-013-0827-3.

Pinder, J. N. (1992) 'Mechanical Noise from Wind Turbines', *Wind Engineering*, 16(3), pp. 158–168.

Raman, G., Ramachandran, R. C. and Aldeman, M. R. (2016) 'A review of wind turbine noise measurements and regulations', *Wind Engineering*, 40(4), pp. 319–342. doi: 10.1177/0309524X16649080.

Shawano County (no date) *Planning and Development, Wind Energy Conversion System*.

Tachibana, H. (2014) 'Outcome of systematic research on wind turbine noise in Japan', *Inter Noise 2014*.

Turnbull CP (2011) 'Measurement of Infrasound from Wind Farms and Other Sources', *Fourth International Meeting on Wind Turbine Noise Rome Italy 12-14 April 2011*.

Vahl, J. *et al.* (2021) 'Infrasound a new weapon in cancer therapy?', *EXPLORE*. doi: 10.1016/j.explore.2021.03.001.

Viterna, L. (1981) 'The NASA-LeRC wind turbine sound prediction code', in *Second DOE/NASA Wind Turbine Dynamics Workshop*. Cleveland.

Viterna, L. (1982) 'Method for predicting impulsive noise generated by wind turbine rotors', in *International Conference on Noise Control Engineering (InterNoise 82)*. San Francisco, pp. 339–342.

Wagn, S., BareiB, R. and Guidati, G. (1996) *Wind Turbine Noise, Paper Knowledge . Toward a Media History of Documents*. Springer.

Walker, B. (2013) 'Infrasound Measurement, Interpretation and Misinterpretation', *5th International Meeting on Wind Turbine Noise Denver 28 – 30 August 2013*.

Watanabe, T. and Møller, H. (1990) 'Low Frequency Hearing Thresholds in Pressure Field and in Free Field', *Journal of Low Frequency Noise, Vibration and Active Control*, 9(3), pp. 106–115. doi: 10.1177/026309239000900303.

Yokoyama, S., Sakamoto, S. and Tachibana, H. (2013) 'Perception of low frequency components contained in wind turbine noise', *Wind Turbine Noise 2013*.

Yount, G. *et al.* (2004) 'Possible Influence of Infrasound on Glioma Cell Response to Chemotherapy: A Pilot Study', *The Journal of Alternative and Complementary Medicine*, 10(2), pp. 247–250. doi: 10.1089/107555304323062239.

Zipp, K. (2012) 'Gears & Gearboxes 101', *Windpower Engineering & Development*.